



**NAVAL
POSTGRADUATE
SCHOOL**

MONTEREY, CALIFORNIA

THESIS

**A LOW-COST, MAN-PORTABLE FREE-SPACE OPTICS
COMMUNICATION DEVICE FOR ETHERNET
APPLICATIONS**

by

Mohammad H. Alrasheedi

December 2005

Thesis Advisor:
Second Reader:

Richard Harkins
Gamani Karunasiri

Approved for public release; distribution is unlimited

THIS PAGE INTENTIONALLY LEFT BLANK

REPORT DOCUMENTATION PAGE			<i>Form Approved OMB No. 0704-0188</i>	
Public reporting burden for this collection of information is estimated to average 1 hour per response, including the time for reviewing instruction, searching existing data sources, gathering and maintaining the data needed, and completing and reviewing the collection of information. Send comments regarding this burden estimate or any other aspect of this collection of information, including suggestions for reducing this burden, to Washington headquarters Services, Directorate for Information Operations and Reports, 1215 Jefferson Davis Highway, Suite 1204, Arlington, VA 22202-4302, and to the Office of Management and Budget, Paperwork Reduction Project (0704-0188) Washington DC 20503.				
1. AGENCY USE ONLY (Leave blank)		2. REPORT DATE December 2005	3. REPORT TYPE AND DATES COVERED Master's Thesis	
4. TITLE AND SUBTITLE: A Low-Cost Man-Portable Free-Space Optics Communication Device for Ethernet Applications			5. FUNDING NUMBERS	
6. AUTHOR(S) Mohammad H. Alrasheedi				
7. PERFORMING ORGANIZATION NAME(S) AND ADDRESS(ES) Naval Postgraduate School Monterey, CA 93943-5000			8. PERFORMING ORGANIZATION REPORT NUMBER	
9. SPONSORING /MONITORING AGENCY NAME(S) AND ADDRESS(ES) N/A			10. SPONSORING/MONITORING AGENCY REPORT NUMBER	
11. SUPPLEMENTARY NOTES The views expressed in this thesis are those of the author and do not reflect the official policy or position of the Department of Defense or the U.S. Government.				
12a. DISTRIBUTION / AVAILABILITY STATEMENT Approved for public release; distribution is unlimited			12b. DISTRIBUTION CODE	
13. ABSTRACT (maximum 200 words) The requirements of modern war have imposed the need for a low-cost, small-size, high-speed, large bandwidth, deployable Free-Space Optics (FSO) system that could be used to provide connectivity between major command centers and their subordinate units. Commercially available FSO systems are bulky and expensive. A preliminary low-cost FSO system was designed, based on commercial off the shelf (COTS) components, and tested over a 5ft. distance in a previous thesis done by Janaka P. Perera. The goal of this thesis is to improve the design and to extend the working range of the FSO. By improving beam collimation, adding precise mechanical movement and using assisting tools and techniques, the FSO network link was successfully established and tested over larger distances using 100Mbps. The maximum distance that could be achieved, with the on-hand optics and a 1mW transceiver, was 40m. Further calculations showed that the FSO link could be established over a 340m distance by using a 3mW transmitter and a 1-inch focuser in the receiver side.				
14. SUBJECT TERMS Free-Space Optics (FSO), Ethernet communicator, Laser Communicator, Fast-Ethernet Device.			15. NUMBER OF PAGES 85	
			16. PRICE CODE	
17. SECURITY CLASSIFICATION OF REPORT Unclassified	18. SECURITY CLASSIFICATION OF THIS PAGE Unclassified	19. SECURITY CLASSIFICATION OF ABSTRACT Unclassified	20. LIMITATION OF ABSTRACT UL	

THIS PAGE INTENTIONALLY LEFT BLANK

Approved for public release; distribution is unlimited

**A LOW-COST MAN-PORTABLE FREE-SPACE OPTICS COMMUNICATION
DEVICE FOR ETHERNET APPLICATIONS**

Mohammad H. Alrasheedi
Lieutenant Commander, Royal Saudi Naval Forces
B.S.EE, King Saud University, 1992

Submitted in partial fulfillment of the
requirements for the degree of

MASTER OF SCIENCE IN APPLIED PHYSICS

from the

**NAVAL POSTGRADUATE SCHOOL
December 2005**

Author: Mohammad H. Alrasheedi

Approved by: Richard Harkins
Thesis Advisor

Gamani Karunasiri
Second Reader

James H. Luscombe
Chairman, Department of Physics

THIS PAGE INTENTIONALLY LEFT BLANK

ABSTRACT

The requirements of modern war have imposed the need for a low-cost, small-size, high-speed, large bandwidth, deployable Free-Space Optics (FSO) system that could be used to provide connectivity between major command centers and their subordinate units. Commercially available FSO systems are bulky and expensive. A preliminary low-cost FSO system was designed, based on commercial off the shelf (COTS) components, and tested over a 5ft. distance in a previous thesis done by Janaka P. Perera. The goal of this thesis is to improve the design and to extend the working range of the FSO. By improving beam collimation, adding precise mechanical movement and using assisting tools and techniques, the FSO network link was successfully established and tested over larger distances using 100Mbps. The maximum distance that could be achieved, with the on-hand optics and a 1mW transceiver, was 40m. Further calculations showed that the FSO link could be established over a 340m distance by using a 3mW transmitter and a 1-inch focuser in the receiver side.

THIS PAGE INTENTIONALLY LEFT BLANK

TABLE OF CONTENTS

I.	INTRODUCTION.....	1
II.	BACKGROUND AND RELATED WORK.....	3
III.	FREE-SPACE OPTICS (FSO) COMPONENTS	9
	A. MEDIA CONVERTER ML6652RDK.....	9
	B. 1X9 TRANSCEIVER.....	12
	C. FIBER OPTICS CABLES	17
	D. COPPER CABLES	22
	E. LENSES	23
	F. FILTERS	25
	G. LASER SAFTY	26
IV.	HISTORICAL OVERVIEW AND SUMMARY OF WORK DONE IN REF. [1].....	29
V.	DESIGN IMPROVEMENT.....	31
	A. STARTING POINT.....	31
	B. STEPS TO EXTEND RANGE AND TESTING	32
VI.	RESULTS AND CONCLUSIONS	37
	A. RESULTS	37
	1. Beam Width Measurement	37
	2. Voltage/Power and Beam Spot Measurements	46
	3. FSO Delay Time Measurements.....	56
	4. Maximum Range Calculation for the Existing FSO System.....	57
	5. Maximum Range Calculation for 3mW Transmitter.....	61
	B. CONCLUSION	63
	LIST OF REFERENCES.....	65
	INITIAL DISTRIBUTION LIST	67

THIS PAGE INTENTIONALLY LEFT BLANK

LIST OF FIGURES

Figure 1.	Fiber Optic Communication System.....	3
Figure 2.	Some of the Commercially Available FSO Equipment (From Ref. [3]).	5
Figure 3.	LightPointe FSO Transceiver (From Ref. [4]).	6
Figure 4.	Modified ML6652RDK Media Converter (From Ref. [1]).	9
Figure 5.	Encoding Schemes. (From Ref. [8]).	10
Figure 6.	FLP Burst.....	11
Figure 7.	Internal Components of a 1x9 Transceiver.....	13
Figure 8.	Transceiver Block Diagram (From Ref. [9]).	13
Figure 9.	Fabry-Perot Laser Diode (After Ref. [10]).	14
Figure 10.	Some TEM Modes (From Ref. [11]).	15
Figure 11.	Gaussian Spherical Beam Propagation in the z Direction (From Ref. [2]).	16
Figure 12.	Multimode Fiber	18
Figure 13.	Conceptual Graded-Index Core (From Ref. [13]).	18
Figure 14.	Single Mode Fiber.....	19
Figure 15.	Attenuation Versus Wavelength in Silica-Based Fiber Optics (From Ref. [15]).	19
Figure 16.	Coupling a Light Source to a Fiber Optics Cable (From Ref. [10]).	20
Figure 17.	Types of Rays Propagating in Fiber Optic Cables (From Ref. [13]).	21
Figure 18.	Interconnection Diagram for UTP Cable (From Ref. [8]).	23
Figure 19.	The Difference in Focusing Capability Between.....	24
Figure 20.	Collimator/Focuser F260FC-C (From Ref. [17]).	24
Figure 21.	Typical Transmission Characteristics <i>FL1300-30 – Laser</i>	26
Figure 22.	Modified ML6652RDK Media Converter (From Ref. [1]).	29
Figure 23.	Initial FSO Link (From Ref. [1]).	30
Figure 24.	Transceivers With Fiber Optics and Lenses to Establish FSO Link Over a 5ft Distance (From Ref. [1])	30
Figure 25.	The FSO System is Anchored on the Test Bench.....	33
Figure 26.	The Two FSO Systems were Mounted on Tripods.....	34
Figure 27.	The Two Systems on Tripods With the Mechanical Rotational Added.	35
Figure 28.	Responsivity vs. Wavelength for InGaAs Detector (From Ref. [17])	38
Figure 29.	Test Arrangement for Beam Width Measurement.....	39
Figure 30.	I-V Characteristics for the InGaAs Photodiode (From Ref. [1]).	39
Figure 31.	Beam Width Measurement.	46
Figure 32.	Test Locations for 5ft Distance.....	47
Figure 33.	F260FC-C Collimator/Focuser (After Ref. [17]).	48
Figure 34.	Test Configuration/Voltage Locations for 3m and Larger Distances.....	49
Figure 35.	Beam Spot for 3m Distance	53
Figure 36.	Beam Spot for 5m Distance.....	53
Figure 37.	Beam Spots for the Two Transmitters at 10m Using a Multimode Fiber Optic Cable.	54

Figure 38.	Beam Spot for the Two Transmitters at 10m Distance Using a Single Mode Fiber.....	55
Figure 39.	Beam Spot for the Two Transmitters at 15m Distance.....	55
Figure 40.	File Process/Transfer Time.....	57
Figure 41.	Maximum Range Calculation for the Existing FSO System.....	60
Figure 42.	Maximum Range Calculation for 3mW Transceiver.....	62

LIST OF TABLES

Table 1.	Recommendation of the Research Team for Wireless Technologies (From Ref. [7]).....	8
Table 2.	Description of the 16 Data Bits in the FLP Burst.	12
Table 3.	Some Types of Connectors Used for Fiber Optic Cables (After Ref. [14]). ...	22
Table 4.	Beam Width Measurement Data for 4mm Distance Between the Transmitter and Detector.	40
Table 5.	Beam Width Measurement Data for 1ft Distance Between the Transmitter and Detector.	41
Table 6.	Beam Width Measurement Data for 2ft Distance Between the Transmitter and Detector.	42
Table 7.	Beam Width Measurement Data for 3ft Distance Between the Transmitter and Detector.	43
Table 8.	Beam Width Measurement Data for 4ft Distance Between the Transmitter and Detector.	44
Table 9.	Beam Width Measurement Data for 5ft Distance Between the Transmitter and Detector.	45
Table 10.	Voltage Measurements for 5ft (1.524m) Distance.	48
Table 11.	Voltage Measurements With and Without the Filter Over 3m and 5m Distances.	50
Table 12.	Voltage Measurements With Multimode and Single Mode Cables Used for Both Transmitters for 10m.	51
Table 13.	Voltage Measurements With and Without Using a Filter Over.	52
Table 14.	Average Process/Transfer Time for Different File Types and Sizes.	56
Table 15.	Advance Calculations to Estimate the Maximum Range for Existing System.	60
Table 16.	In Advance Calculations to Estimate the Maximum Range for a 3mW Transmitter.	61
Table 17.	In Advance Calculations to Estimate the Maximum Range for a 3mW Transmitter and a 1-inch Receiver Focuser.	63

THIS PAGE INTENTIONALLY LEFT BLANK

ACKNOWLEDGMENTS

The author would like to acknowledge SPAWAR System for the financial support of this project.

The author is grateful to the following individuals for their support and guidance during his research and learning:

Prof. Gamani Karunasiri, Physics Dept.

Prof. Richard Harkins, Physics Dept.

Mr. Sam Barone, Physics Dept.

Mr. George Jaksha, Physics Dept.

THIS PAGE INTENTIONALLY LEFT BLANK

EXECUTIVE SUMMARY

The Free-Space Optics (FSO) system has gained popularity in recent years in civilian and military applications as a solution for the “last mile problem” and as a low cost way to connect major command and control networks with their subordinates in the field. The commercially available FSO systems are bulky and expensive.

A preliminary Free-Space Optics (FSO) device was designed, from commercial off the shelf (COTS) components, and tested over a 5ft distance in a previous thesis by Janaka P. Perera. In this thesis the working distance for the FSO system was extended to 40m using small laser collimators and a 1mW FP laser diode transmitter. Successful data transfer, via FSO link, was demonstrated between two laptops using a 100Mbps data rate. Further calculation showed that the range could be extended to 340m by using a 3mW transmitter and 1-inch focuser in the receiver side. Further distances could be achieved by using more powerful transmitters.

The most challenging problem in this project is to facilitate the alignment process, which could be done by using a large-diameter collimator and powerful transmitter so that the beam could be spread widely, at the receiver location, with enough power to overcome the receiver threshold.

THIS PAGE INTENTIONALLY LEFT BLANK

I. INTRODUCTION

Using light for free-space communications has gained popularity, in recent years, as an alternative to conventional radio frequency methods. The main reasons behind the interest in light communication are speed and large bandwidth. Fiber optics cables are widely replacing coaxial and bulky radio/microwave equipment with high-speed, secure, and relatively low-cost media. Fiber optics has solved the bandwidth limitation in large computer networks where it is cost effective to use fiber optics cables. With the increase in distributed computer applications and individual dependency in computer networks as a source of information, the requirement to extend the high bandwidth and speed of fiber optics to the end user has appeared. This is commonly referred to as the “last mile problem.” One of the solutions to this problem is found in Free-Space Optics Communications (FSO). FSO has gained popularity in recent years in both civilian and military fields.

The objective of this thesis is to improve the design, test and evaluate a competitive low-cost, man-portable, Free-Space Optics (FSO) communication device that could be used to improve the mobility and performance of tactical networks in USN.

This thesis is organized as follows:

- Chapter II covers the background and related work. It provides information and background about other research done in the FSO area.
- Chapter III describes the components of the designed FSO system, and it covers the theory of operation of these components and provides the necessary theoretical background that may help understand the work done in this thesis.
- Chapter IV is an historical overview and summary of the previous work done in [1].
- Chapter V covers the work done to improve the FSO system design.
- Chapter VI includes the test results and the author’s conclusions and recommendations.

THIS PAGE INTENTIONALLY LEFT BLANK

II. BACKGROUND AND RELATED WORK

As the dependency on using computer networks as a source of information increases, the need to expand the network also increases, and the need of high-speed connectivity between computers and between networks largely increases. With the large expansion of networks and the increased demand of using more applications that require large bandwidth, the traditional copper cables reached their capacity limits and a need has arisen to replace the traditional copper cables with other types of connectivity, like fiber optics and radio waves.

Nowadays, fiber optics are rapidly replacing copper cables and microwave connectivity, not only because of the high-speed and large bandwidth, but also because fiber optics are more secure, take less space and are immune to electromagnetic interference. Figure 1 shows the essential components for fiber optics communications.

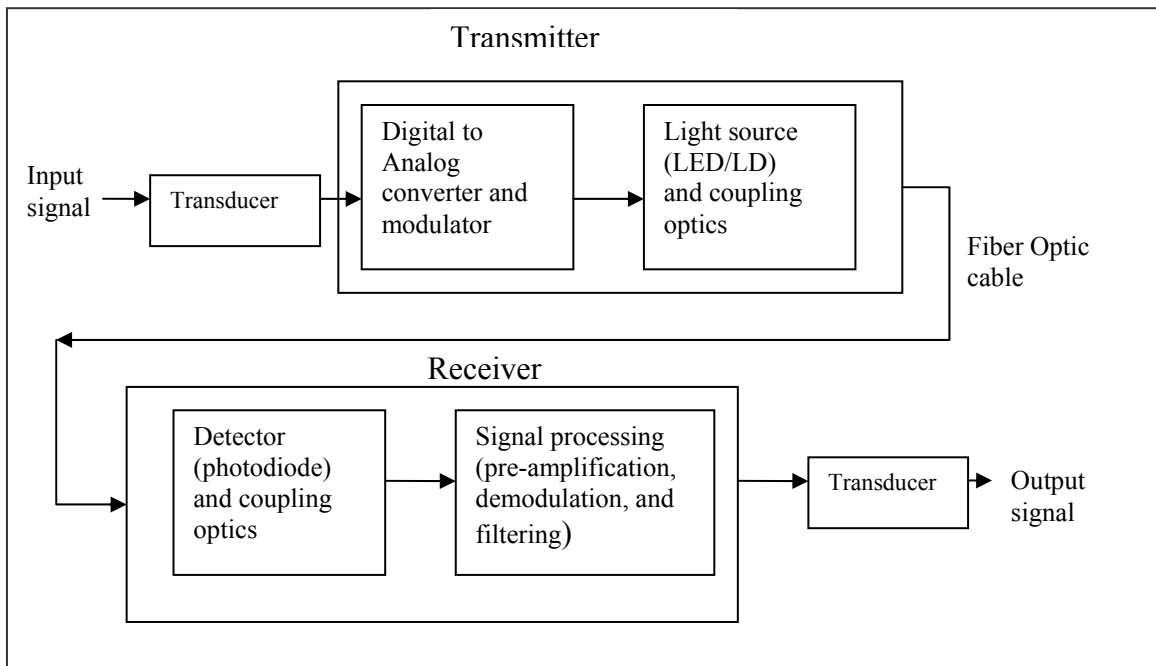


Figure 1. Fiber Optic Communication System

As shown in Figure 1, the base-band input signal is converted by a transducer to an analog electrical signal. The analog signal is then converted to a digital signal and modulated. In order to transmit a signal via fiber optic cable, it has to be converted to light.

To couple light to the fiber optic cable an optical transducer and coupling devices are used. At the receive side, a reverse process occurs to reconvert the signal back to an electrical signal. These are the basic components of the fiber optic communication system.

The capacity of any communication channel is proportional to the bandwidth of its frequency band. Light has extremely large bandwidth, which means it can carry many more times the information now carried by radio waves or coaxial cables. For example, the center frequency for the visible light spectrum is 10^5 times greater than the frequency of 6cm microwave system. Hence, theoretically the information capacity of typical light is 10^5 times greater than that of a typical microwave. A telephone call requires about 3.8kHz of frequency band. It can be carried by coaxial cable (10^6 bandwidth) and occupy 0.4% of its bandwidth. However, if a He-Ne laser, 632.8nm 4.738×10^{14} Hz, is used it will occupy less than one billionth of 1% of the available laser beam frequency [2].

Fiber optics has solved part of the bandwidth limitation problem between large networks, where it is cost effective; but it was not the complete solution, because the problem still exists in the last mile, where the paths leading to homes and offices are located. In the last mile, copper cables are still creating a bottleneck problem.

In recent years, the interest in having a Free-Space Optics (FSO) communications system has grown rapidly in the military and civilian fields as point-to-point communications between fixed sites. Many companies have been using FSO equipment to provide Internet subscribers with high-speed connections, up to 2.5Gbps, for a distance of more than 4Km and with a very low bit error rate (BER). FSO addresses the “last mile problem” in a cost effective way. It avoids the high cost of fiber and the hassle of getting RF spectrum licenses. Figure 2 shows some of the commercially available FSO equipment.



Figure 2. Some of the Commercially Available FSO Equipment (From Ref. [3]).

The commercially available FSO is a wireless line-of-sight communication between two points. This type of communication can handle data at a rate of more than 1Gbps over a distance that may reach more than 4km. FSO was originally developed to solve the “last mile problem” bottleneck with a cost effective way that avoids the high cost of fiber optic cables.

FSO has many advantages over the existing types of communications that make this type of communication attractive in civilian and military fields:

- Large bandwidth.
- Spectrum licensing is not required.
- Easy and fast to install.
- Low bit error rate.
- Low power consumption.
- Relatively low cost when compared with cables, microwave and radio transceivers.

FSO has been used widely to connect Internet subscribers and networks. Nowadays, many FSO transceivers are commercially available.

The commercially available unit is composed of a light source, a photo-detector, coupling lenses or telescope, and auto alignment equipment. Figure 3 shows one of the commercially available FSO transceivers used to connect Internet sub-networks. This transceiver can be mounted on the roofs of buildings. Most of the FSO transceivers use a laser diode as a light source, so that they are available to work at wavelengths of 850, 1310, or 1550 nm.

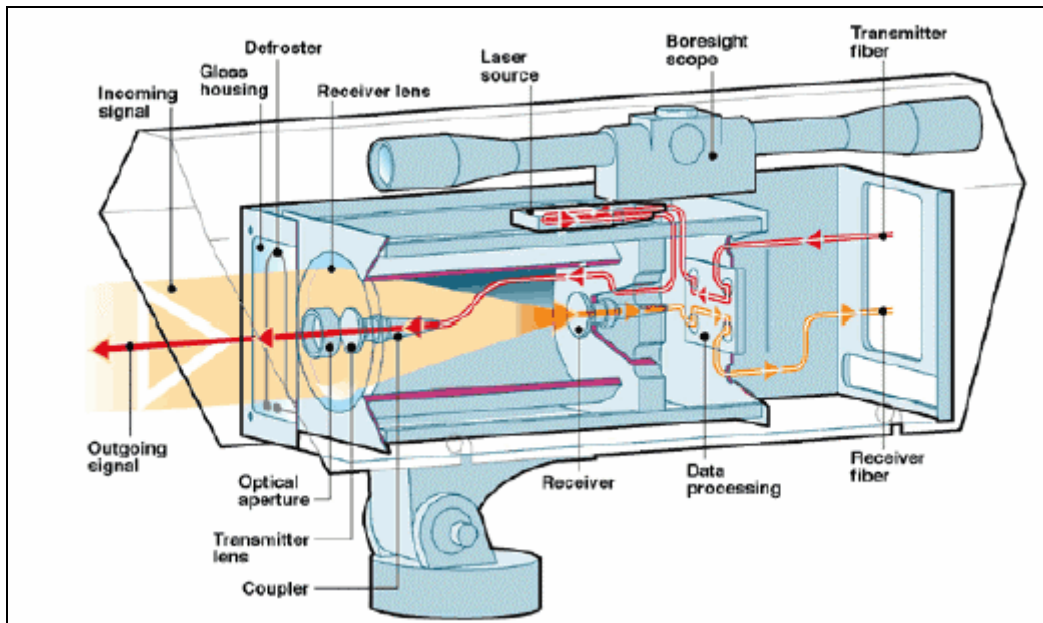


Figure 3. LightPointe FSO Transceiver (From Ref. [4]).

These commercially available FSO transceivers have a relatively high cost, typically between \$5,000 and \$50,000.

Additionally, FSO has other advantages that draw the attention of the military; such as small-size, security, and immunity to electromagnetic interference (EMI) (for more information on this subject see Ref. [5]). A considerable amount of research has been done during the last decade to implement FSO systems in the United States Navy. Lucent technologies has demonstrated a successful shipboard implementation and test for FSO in San Diego during the period of February 11, 1999 to March 23, 1999 [6]. The U.S. Naval Research Laboratory (NRL) has conducted several successful experiments on the FSO

system between Chesapeake Bay, MD, and Tilgman Island, MD, over a distance of 34.4Km with 622Mbps and a bit error rate (BER) less than 10^{-6} [6].

Also, a field test with government contractors and private vendors has been conducted to demonstrate the capabilities of various wireless systems used in (1) Unit Operations Center (UOC), (2) Common Aviation Command and Control System (CAC2S), and (3) Command and Control On-the-Move Network Digital Over-the-Horizon Relay (CoNDOR). The recommendations of the team on how to best implement these technologies for UOC, CAC2S, and CoNDOR are given in Table 1. FSO, one of the wireless technologies researched by this team, Table 1, was recommended for use in LOS intra-nodal connections for UOC, CAC2S and CoNDOR, and it has been found that FSO is the right fit for short distances of less than 2Km [7].

Since an FSO system will be used to improve the mobility and performance of tactical networks, this system needs to be small in size, low-cost, portable and reliable. Is it possible to make a small and cost effective FSO device that satisfies these requirements? The answer is the subject of this thesis.

UAC/CACS	FSO	MCROWAVE	802 16	OFDM	BROADBAND SATELLITE	INMARSAT	IRIDIUM	80211b over SecNet- 11
INTRA-NODAL								
LOS	1	2	4	3				5
BLOS				1				
INTRA-NODAL								
LOS	4	3	2	1				5
BLOS				1	2	3	4	
OTH					1	2	3	
COMMS ON THE MOV								
With in the convoy				1				2
Outside the convoy				3		1	2	
For short/long halts, refer to intra-Nodal BLOS/OTH section								
AERIAL RELAY (UAVBALOON)				2				1
CoNDOR	FSO	MCROWAVE	802 16	OFDM	BROADBAND SATELLITE	INMARSAT	IRIDIUM	80211b over SecNet- 11
INTOPOP-V								
LOS	1	2	4	3				5
BLOS				1	2	3	4	
OUT OF POP-V TO MBC								
BLOS				1	2	3	4	
OTH					1	2	3	
COMMS ON THE MOV								
With in the convoy				1			3	2
Outside the convoy				3		1	2	
For short/long halts(BLOS)				1	2	3	4	
AERIAL RELAY (UAVBALOON)				2				1
Ranking of technologies for each program (1=first recommendation, 2=second recommendation...)								

Table 1. Recommendation of the Research Team for Wireless Technologies (From Ref. [7]).

III. FREE-SPACE OPTICS (FSO) COMPONENTS

The components of the FSO system used in this project are:

- Media converter ML6652RDK.
- 1x9 Transceiver.
- Fiber optics cables.
- Copper cables.
- Lenses.
- Filters.

These components are described in detail in the following sections.

A. MEDIA CONVERTER ML6652RDK

The Media converter is a device that converts an electrical signal to a light signal and vice versa. In this project, the ML6652RDK from Micro Linear was used. This media converter originally comes with an Agilent HFBR-5103 transceiver, which operates at a wavelength of 1300nm with an LED of output power 0.04mW (-14dB). Because the transceiver is designed to be used with fiber optic cables, it is not suitable to be used in FSO communications. It was removed, as described in [1], and a 1x9 connector was left in place, to be used for another higher power laser transceiver. The modified ML6652RDK is shown in Figure 4.



Figure 4. Modified ML6652RDK Media Converter (From Ref. [1]).

The media converter operates at 10/100Mbps data throughput rates and supports standard Ethernet protocols at the data link layer. It also supports the Auto-Negotiation

feature using signals at wavelengths of 850nm or 1310nm. It is provided with an RJ45 port as a connector to UTP (Universal Twisted Pair) copper cables.

Two LEDs located near the transceiver are used to illuminate when successful link negotiation at 100Mbps or 10Mbps is achieved. It also has two built-in LEDs in the RJ45 connector, one is yellow and the other is green. The green LED will be lit when there is traffic on the UTP side and the yellow LED will be lit when there is traffic on the fiber optic side of the link.

In order to reduce the effect of noise, signal distortion, and to eliminate the need for clocking, the data is encoded before transmission over UTP or fiber optics using the Manchester code for 10 Mbps, and 4B5B and MLT-3 (Multilevel Transmission Encoding - 3 levels) for 100Mbps. In Manchester encoding, the bit 1 is represented as a low-to-high transition at the middle of the bit, and the bit 0 is represented as a high-to-low transition at the middle of the bit. Manchester encoding uses 20Mbaud to represent 10Mbps, and for this reason this type of encoding is not efficient to for higher bit rates. In 4B5B encoding, 4-bit nibbles are encoded as 5-bits, which will result in 125Mbaud for the 100Mbps. The MLT-3 scheme concentrates most of the transmitted power below 30 MHz, which reduces electromagnetic radiation. The encoding schemes are shown in Figure 5.

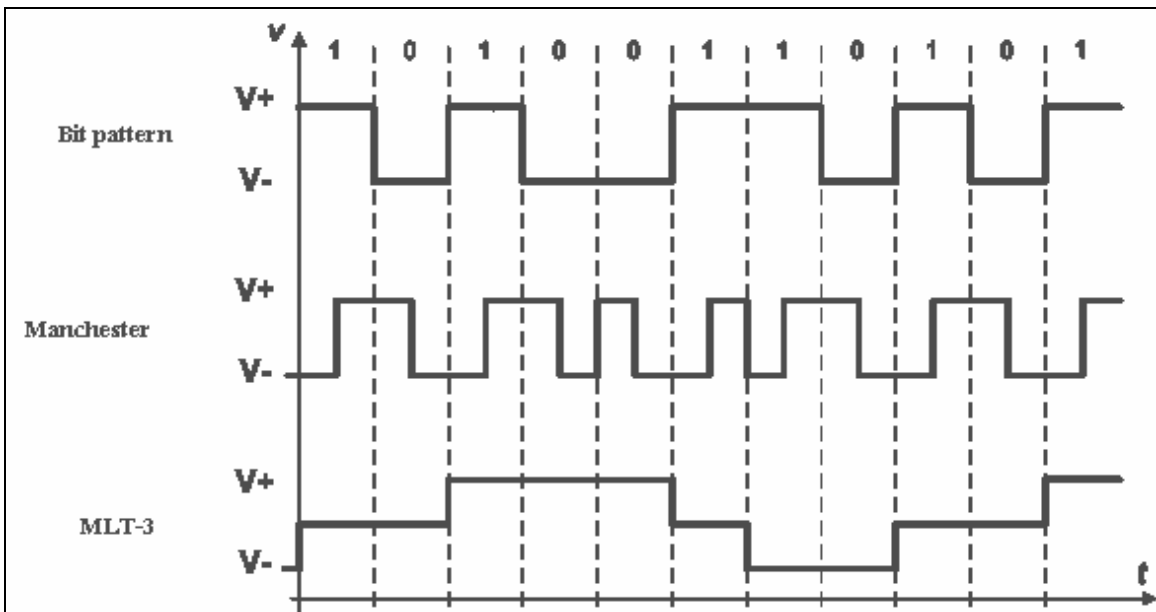


Figure 5. Encoding Schemes. (From Ref. [8]).

The auto-negotiation process is a feature that enables the device to automatically establish a link with other remote devices in 10 or 100Mbps, in either half or full duplex modes. During the auto-negotiation process the device transmits FLPs (Fast Link Pulses) which are a sequence of NLPs (Normal Link Pulses) used in 10Base-T. The FLP bursts are transmitted each 16ms +/- 8ms with width of 2ms. The FLP burst is shown in Figure 6.

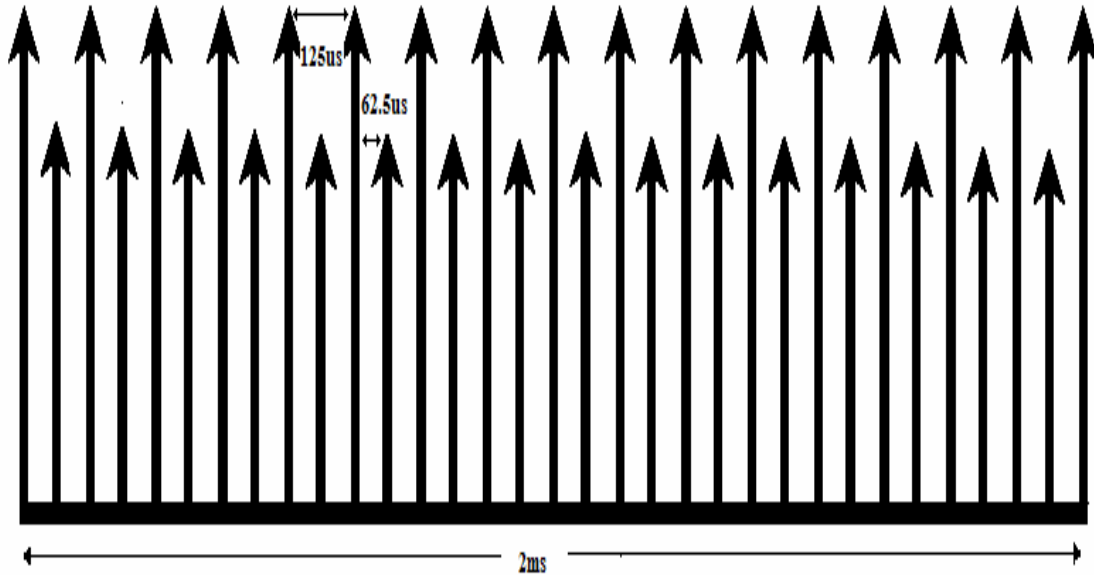


Figure 6. FLP Burst

Each FLP burst consists of 17 clock pulses interleaved with 16 data pulses. The 16 data pulses contain all the information about the bit rate to be used. The data pulses are shown in Table 2.

Bit 0 to Bit 4	Selector Field bits : Defines the used technology
Bit 5	10 Base-T Half Duplex
Bit 6	10 Base-T Full Duplex
Bit 7	100 Base-TX Half Duplex
Bit 8	100 Base-TX Full Duplex
Bit 9	10 Base-T4
Bit 10	Pause
Bit 11	Asynchronous Pause
Bit 12	Not Defined
Bit 13	Remote Fault
Bit 14	Acknowledge
Bit 15	Next Page

Table 2. Description of the 16 Data Bits in the FLP Burst.

B. 1x9 TRANSCEIVER

The transceiver used in the FSO system is a 1x9 pin package transceiver from Lasermate Group, Inc., with part number C13F-155SCL5 (new part No. CS13F-03A-5LPC-C). It operates at a wavelength of 1310nm with Fabry-Perot laser transmitter output power between 0 and -5dB (1mW and 316 μ W respectively). The receiver has a sensitivity of less than -30dB which means it can detect power less than 1 μ W using 1mW reference. It uses a duplex SC (Subscription Channel Connector) fiber connector and 5Volt power supply. Figure 7 shows the internal components and Figure 8 shows a block diagram of a 1x9 transceiver. The transceiver consists mainly of the TOSA (Transmitter Optical Sub Assembly), the ROSA (Receiver Optical Sub Assembly) with a Trans-Impedance Amplifier (TIA), a PECL (positive-referenced emitter-coupled logic) laser driver, a limiting amplifier, a signal conditioning, and a post amplifier. The laser driver converts Positive Emitter Coupled Logic (PECL) data to bias the current and provide modulation for the FP laser diode. The ROSA incorporates an efficient InGaAs PIN photo-diode which converts the light signal into an electrical current. This signal is amplified and regenerated into PECL-compatible data by the trans impedance amplifier (TIA).

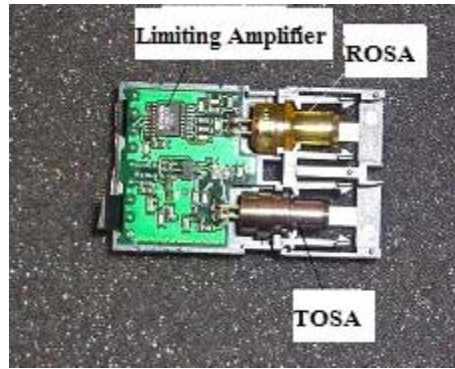


Figure 7. Internal Components of a 1x9 Transceiver.

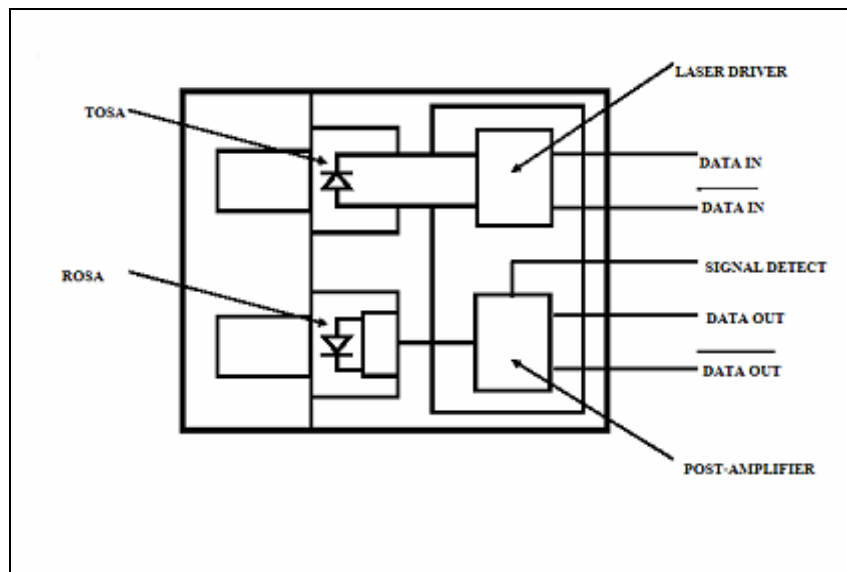


Figure 8. Transceiver Block Diagram (From Ref. [9]).

The Fabry-Perot laser diode is shown in Figure 9. This laser diode consists of two partially reflecting mirrors facing the cleavage plane of a crystal with stimulated emitted rays confined between the reflecting mirrors. The stimulated emitted rays use the cavity to travel back and forth between the two mirrors forming a standing wave until they exit from the device.

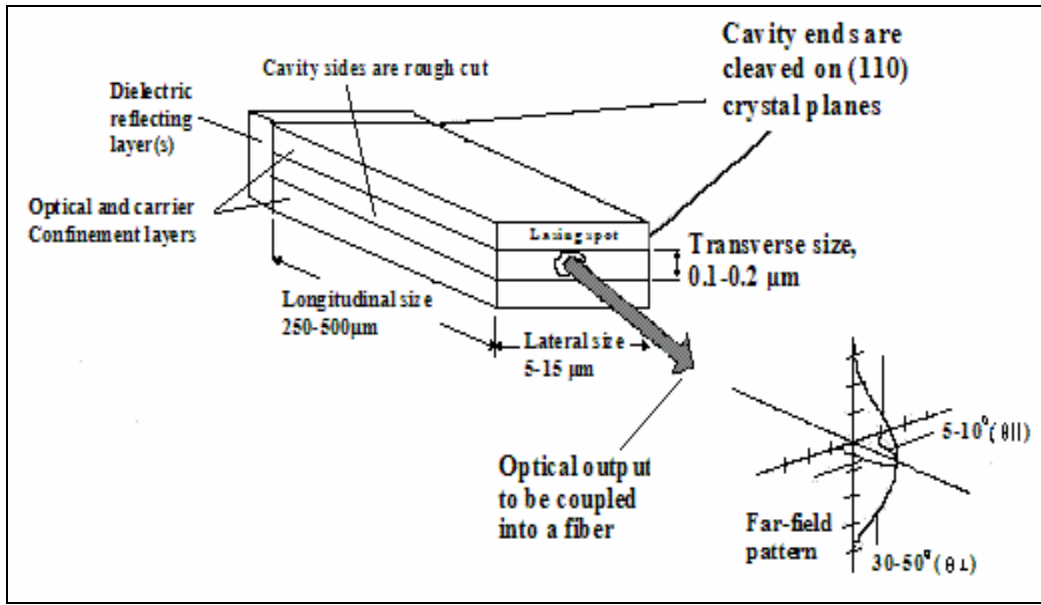


Figure 9. Fabry-Perot Laser Diode (After Ref. [10]).

The FP laser transmits coherent light using the fundamental transverse electromagnetic mode ($TEM_{0,0}$), which has the smallest spot size, the lowest divergence, and its output intensity is distributed as a Gaussian function. The output beam is a three-dimensional Gaussian function with divergence angles $\theta_{\perp} = 15 - 30^\circ$ and $\theta_{\parallel} = 30 - 50^\circ$. This large divergence angle is suitable for coupling the beam to fiber optics cables, but it is not suitable for free-space transmission because the beam will spread rapidly over a large area and disappear after a few centimeters. In order to use such a beam in free-space transmission, a collimator will be used to reduce the divergence angle and to increase the distance that can be reached by the beam.

Some of the TEM modes and their associated electric field waveforms and beam spots are shown in Figure 10.

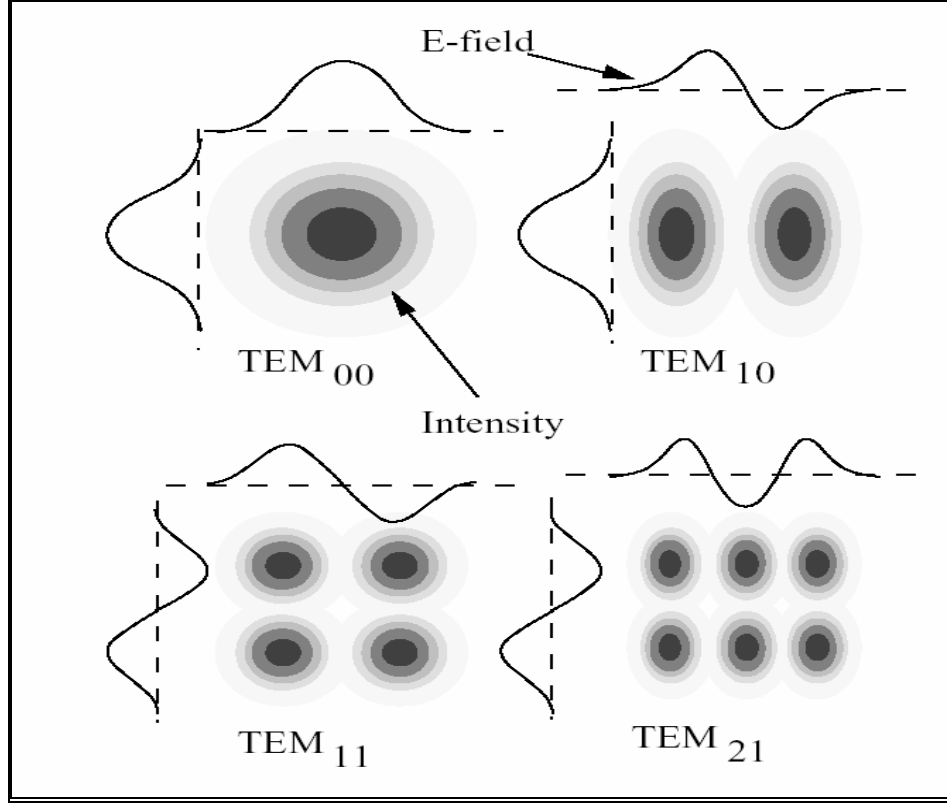


Figure 10. Some TEM Modes (From Ref. [11]).

In Figure 10 the TEM_{00} is composed of concentric circles that represent different irradiances or intensities. The intensity decreases gradually from the center to the edges. The beam diameter is defined as the width of the Gaussian function when the irradiance equals $1/e^2$ of the maximum irradiance ($1/e^2 = 0.135$). The spot size or the beam waist ($w(z)$) of the beam is the radius of the circle measured from the center point of maximum irradiance to the $1/e^2$ point. The propagating waves start as plane waves at the beam waist (w_0). As the distance from the source increases, the divergence angle increases, the beam waist (spot size) increases, and the curvature of the wave increases. Equation 3.1 and equation 3.2 can be used to compute the beam waist and radius of curvature ($R(z)$), respectively [2].

$$w(z)^2 = w_0^2 \left[1 + \left(\frac{\lambda z}{\pi w_0^2} \right)^2 \right] \quad 3.1$$

$$R(z) = z \left[1 + \left(\frac{\pi w_0^2}{\lambda z} \right)^2 \right] \quad 3.2$$

where z is the distance from beam waist location, w_0 is the spot size at the beam waist, and λ is the operating wavelength.

At the far field when $z \gg \frac{\pi w_0^2}{\lambda}$, the above equations can be approximated to the following forms [2]:

$$R(z) = z \quad 3.3$$

$$w(z) = \frac{\lambda}{\pi w_0} z \quad 3.4$$

Hence the half-angle beam divergence is given by the following equation [2]:

$$\theta \cong \frac{\lambda}{\pi w_0} \quad 3.5$$

Figure 11 shows all these parameters and how the irradiance decreases as the beam propagates away from the light source.

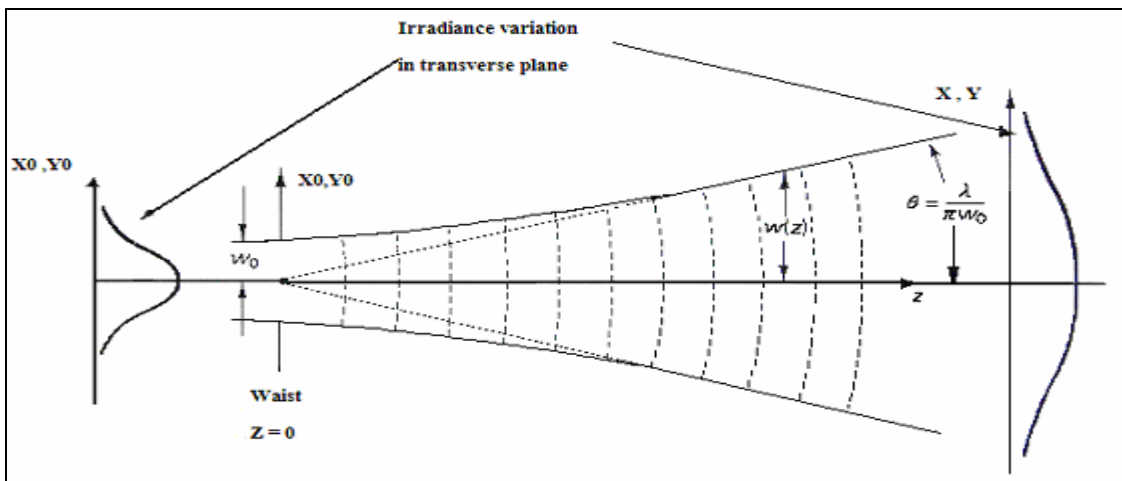


Figure 11. Gaussian Spherical Beam Propagation in the z Direction (From Ref. [2]).

As the beam waist increases, the beam spot size becomes larger than the receiver aperture and that results in geometric losses.

In addition to the beam spread, the beam power is attenuated also as it travels in free-space. If P_T is the transmitted power, then the received power, P_R , at a distance R from the transmitter will be given by equation 3.6 [10]:

$$P_R = P_T e^{-\alpha R} \quad 3.6$$

where α is the atmospheric attenuation coefficient.

The atmospheric attenuation, beam divergence angle and the geometric losses can be combined in one equation as given by equation 3.7 [12]:

$$P_R = P_T \frac{A_{receiver}}{(\theta R)^2} e^{-\alpha R} \quad 3.7$$

where θ is the divergence angle of the beam.

C. FIBER OPTICS CABLES

Fiber optics are fibers of glass or plastic that carry light for long distances, up to 50km, without need of repeaters. There are two major types of fiber optic cables, single mode and multimode. The multimode fibers have diameters in the range of 50-100 μm , while single mode fibers have diameters in the range of 2-8.3 μm . The most commonly used cables are: single mode fiber of 9/125 μm and multimode fiber of 62.5/125 μm , where the first number is the core diameter and the second is the cladding diameter.

The larger diameter in multimode fibers permits more modes to propagate along the fiber due to reflection of light in different angles. Some reflected rays will follow longer paths than others, and hence arrive later to the receiver. Rays going in straight lines will arrive first. This difference in arrival times/paths of reflected rays could cause a problem called modal dispersion. This problem results in a distorted signal in the receiver side in long cables (greater than 3000ft). Hence, the multimode fiber is used for short distances with much easier alignment than the single mode fiber. The typical wavelengths used in multimode are 850 or 1300nm. The multimode fiber is shown in Figure 12.

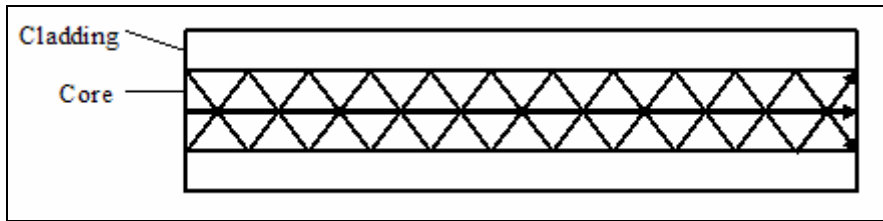


Figure 12. Multimode Fiber

One way to eliminate the modal dispersion problem in the multimode fiber is by using a Graded Index (GRIN) fiber where the fiber core index of refraction gradually decreases from the core axis as a function of the radius. The core consists of a series of concentric cylinders with different refractive indexes that work to reflect the rays toward the core axis. Figure 13 shows a conceptual graded index core.

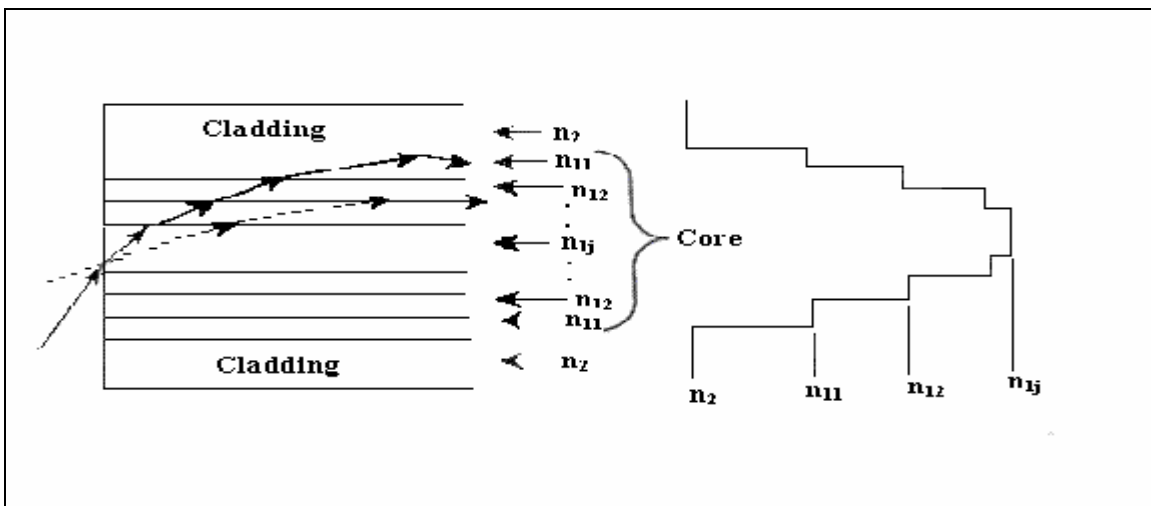


Figure 13. Conceptual Graded-Index Core (From Ref. [13]).

Another way to eliminate the modal dispersion is to reduce the core's diameter until the fiber allows only one mode to propagate. The type that uses this approach is called the single mode fiber, which has higher bandwidth, speed, and up to 50km transmission distance. The typical wavelength of light used in single mode fibers is 1310 or 1550nm. A single mode fiber is shown in Figure 14.

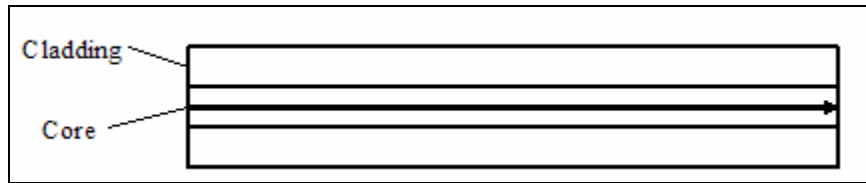


Figure 14. Single Mode Fiber.

The operating wavelengths in silica-based fiber optics are divided into five windows. The first window, which operates at a wavelength around 850nm, was used in the early developed fibers and became less attractive because of its relatively high loss (3dB/km) loss limit [13]. The second window operates at a wavelength around 1310nm with attenuation of around 0.5dB/km. The third window of wavelength was developed in late 1977 by Nippon Telegraph and Telephone (NTT), and operates at 1550nm with attenuation around 0.2dB/km [14]. The fourth window with a wavelength around 1620nm, and the fifth window are under development. Figure 15 shows the attenuation of the five wavelength windows [15].

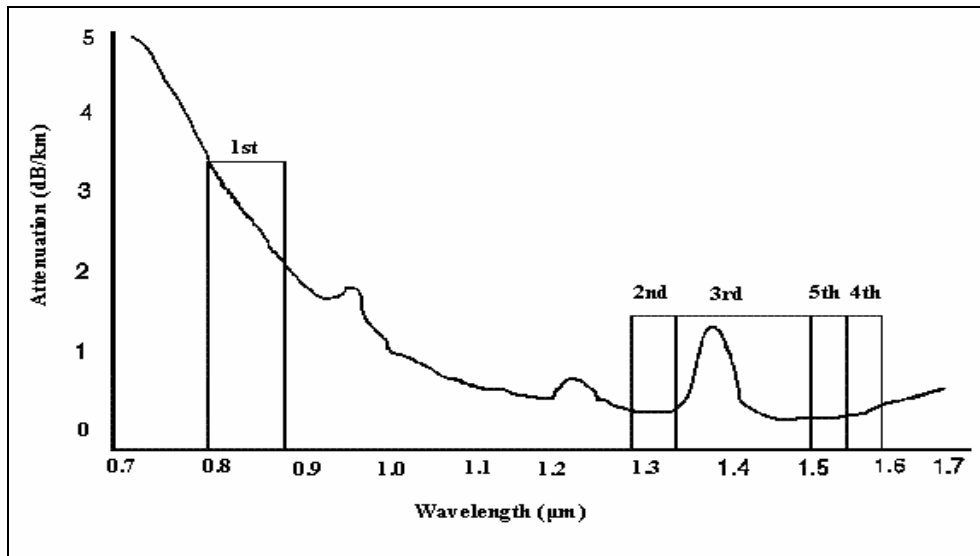


Figure 15. Attenuation Versus Wavelength in Silica-Based Fiber Optics (From Ref. [15]).

Systems that use wavelengths of 850nm, 1310nm, and 1550nm, along with the visible wavelength of 660nm, are manufactured today. Long wavelength is more costly than the short wavelength.

Light is coupled into fiber either directly or using a focuser. The coupling efficiency depends on a number of parameters like the output optical power, area of the light source, the fiber acceptance angle (the type of the fiber), and the losses due to reflections/scattering. This is illustrated in Figure 16. Most of the focuser/collimators provide 75%-85% coupling efficiency for multimode fibers and 35%-65% for single mode fibers.

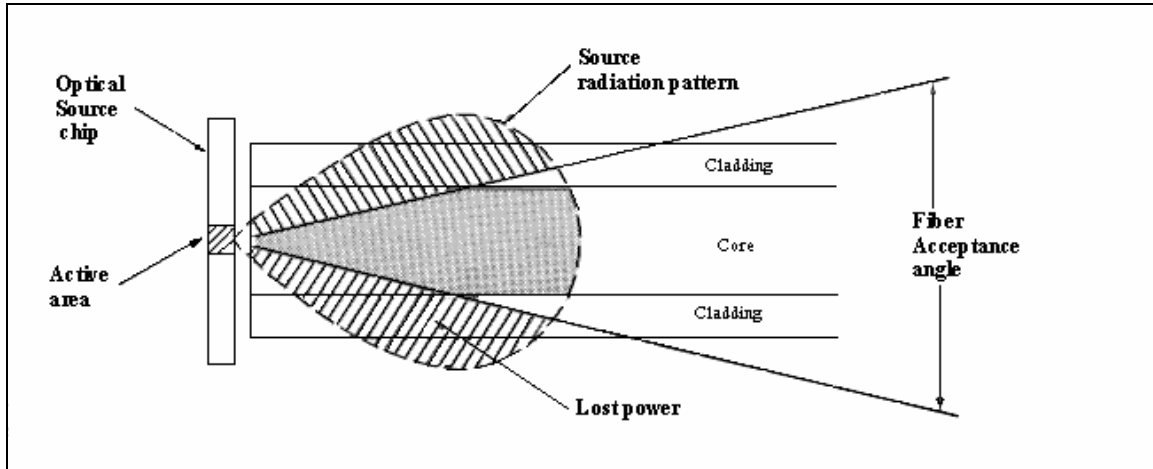


Figure 16. Coupling a Light Source to a Fiber Optics Cable (From Ref. [10]).

The light beam will be bounded in the fiber if the launching angle is greater than the critical angle. The critical angle for a fiber optic cable surrounded by air ($n_0 = 1$) is obtained from the following equation [2]:

$$\theta_c = \sin^{-1}(n_2 / n_1). \quad 3.8$$

The number of modes propagating in fiber optics is determined by V parameter, which is given by [16]:

$$V = \frac{2\pi a}{\lambda_0} (n_1^2 - n_2^2)^{\frac{1}{2}} \quad 3.9$$

where a is the core radius, n_1 is the core refractive index and n_2 is the cladding refractive index. If $V < 2.405$ only one mode will propagate, and if $V > 1$ the number of modes is given by:

$$N \cong \frac{V^2}{2} \quad 3.10$$

The numerical aperture (NA) of the fiber and the fiber acceptance angle (α_{\max}) are given by the following equations [16]:

$$NA = n_0 \sin \alpha_{\max} = (n_1^2 - n_2^2)^{\frac{1}{2}} \quad 3.11$$

$$\alpha_{\max} = \sin^{-1}(NA / n_0) \quad 3.12$$

where n_0 is the surrounding refractive index.

Depending on the launching angle, the rays traveling in the fiber optic cable can be divided into three types: meridional rays, axial rays, and skew rays. Meridional rays are rays that pass through the axis of the optical fiber. Axial rays are rays that propagate along the fiber axis. Skew rays are rays that travel through an optical fiber without passing through its axis. Figure 17 shows these types of propagating rays. The acceptance angle for skew rays is larger than the acceptance angle of meridional rays. The presence of skew rays increases the amount of loss in a fiber.

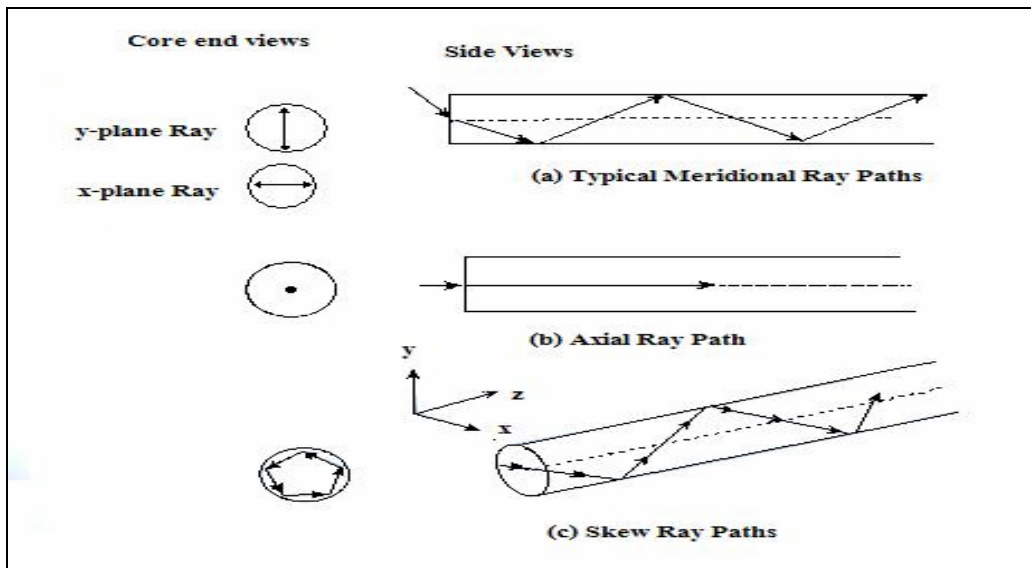


Figure 17. Types of Rays Propagating in Fiber Optic Cables (From Ref. [13]).

To join/align fibers together, or to couple fibers to transmitters/receivers, fiber optics connectors are used. There are many types of connectors used for fiber optics cables. Table 3 shows the most commonly used connectors. All these connectors can be used with multimode or single mode fiber optics cables. The choice of the connector depends on the application.


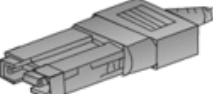
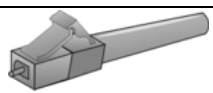
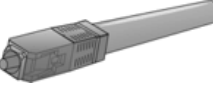
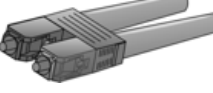

Connector	Insertion Loss	Repeatability	Fiber Type	Applications
 FC	0.50-1.00 dB	0.20 dB	Single mode, Multi mode	Datacom, Telecommunications
 FDDI	0.20-0.70 dB	0.20 dB	Single mode, Multi mode	Fiber Optic Network
 LC	0.15 db (SM) 0.10 dB (MM)	0.2 dB	Single mode, Multi mode	High Density Interconnection
 SC	0.20-0.45 dB	0.10 dB	Single mode, Multi mode	Datacom
 SC Duplex	0.20-0.45 dB	0.10 dB	Single mode, Multi mode	Datacom
 ST	Typ. 0.40 dB (SM) Typ. 0.50 dB (MM)	Typ. 0.40 dB (SM) Typ. 0.20 dB (MM)	Single mode, Multi mode	Inter-/Intra-Building, Security, Navy

Table 3. Some Types of Connectors Used for Fiber Optic Cables (After Ref. [14]).

D. COPPER CABLES

The copper cables used are unshielded twisted-pair cables (UTP) with RJ45 connectors. Category 3 of UTP can support up to 10Mbps, making it suitable for 10BaseT

networks. However, for fast Ethernet (100Mbps and higher), UTP CAT5 or higher UTP categories should be used in order to achieve the maximum distance (100m) specified by the 100BaseTX standard. In this project, CAT5 UTP cables were used to directly connect two computers together, or to connect a computer to the media converter. To connect two computers directly together, a crossover UTP cable should be used. A straight through UTP cable can be used to connect a computer to a Local Area Network (LAN) because the crossover connection is already done at the hub or the router. Figure 18 shows an RJ45 connector pin and interconnection diagram for straight and crossover UTP cables.

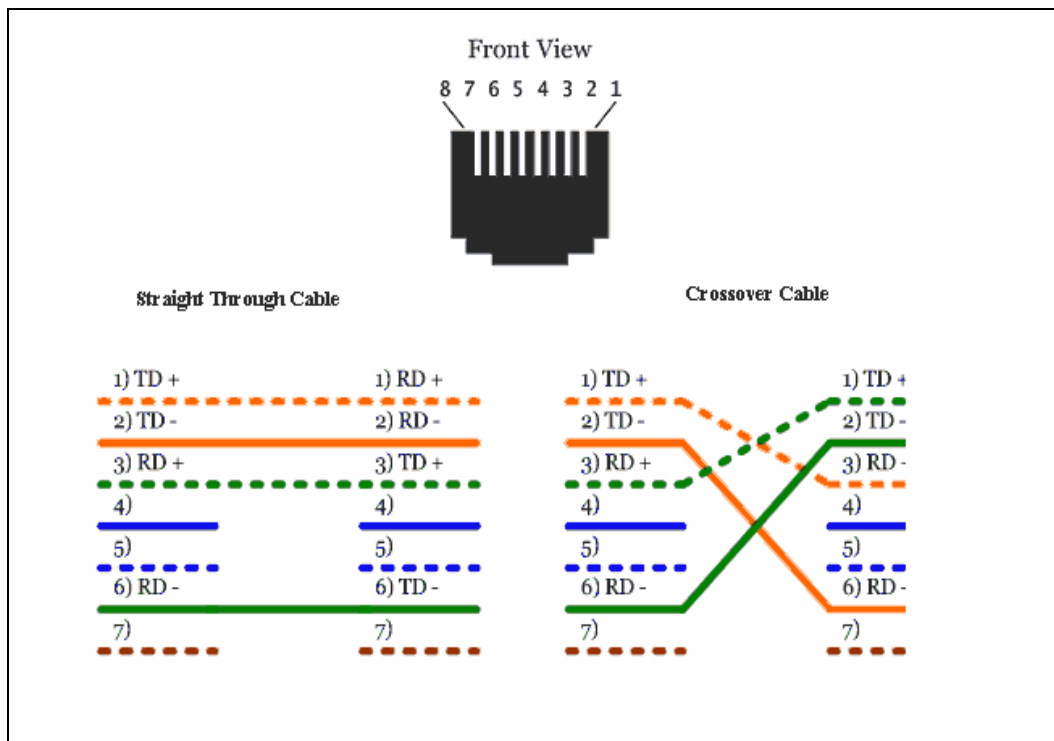


Figure 18. Interconnection Diagram for UTP Cable (From Ref. [8]).

E. LENSES

There are many types of lenses to choose from for an FSO application: (1) Ball lenses, (2) Aspherical lenses, (3) Spherical lenses, (4) GRIN (GRAded INdex) lenses, and (5) Cylindrical lenses. These lenses may be manufactured from glass, plastic or silicon. Commonly used lenses in optical communications are the GRIN, spherical, and aspherical lenses. However, the most common is the aspherical lens, which has less scattering than the

spherical lens and can be focused precisely using fewer numbers of lenses. Figure 19 shows the difference between spherical and aspherical lenses in focusing light.

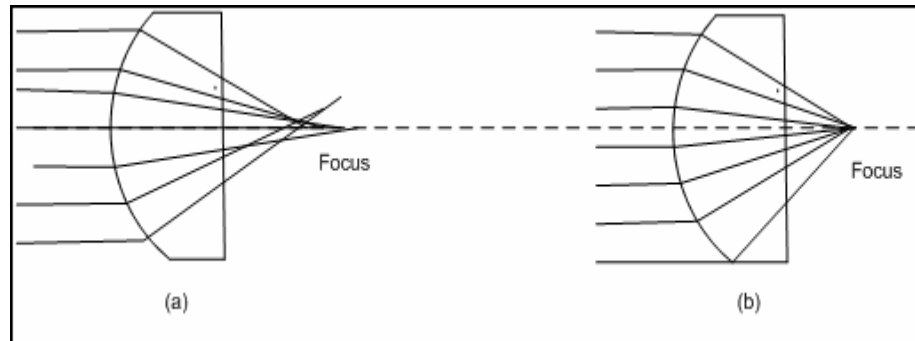


Figure 19. The Difference in Focusing Capability Between (a) Spherical Lens and (b) Aspherical Lens.

In this FSO system, the lenses used were four small aspherical lenses from Thorlabs, Inc. Actually they are light collimators/focusers (Part No. F260FC-C), with a diameter of about 7mm. They operate in the wavelength range of 1050-1550nm. This collimator is shown in Figure 20.

These collimators/focusers have a focal length of 15.29mm, an output beam diameter $\frac{1}{e^2} \approx 2.74\text{mm}$, and full-angle beam divergence of 0.035° at wavelength 1310nm [17].

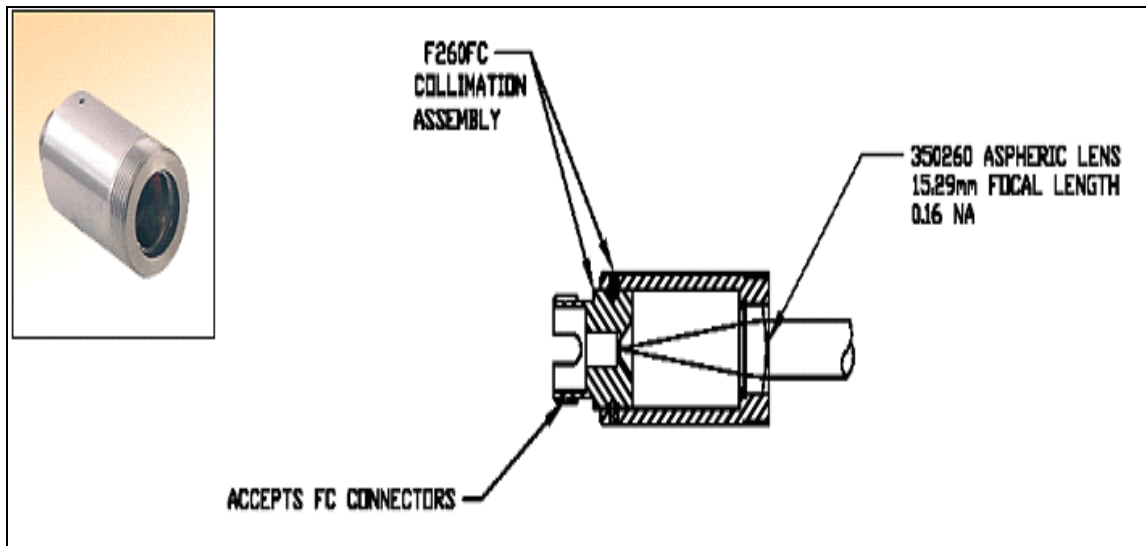


Figure 20. Collimator/Focuser F260FC-C (From Ref. [17]).

The relations between the beam waist, beam diameter, focal length and numerical aperture are given by equations 3.13 and 3.14 [18]:

$$\text{Beam Diameter} = 2w(z) = 2 \times f \times NA \quad 3.13$$

$$\theta(\text{mrad}) = \frac{a(\mu\text{m})}{f(\text{mm})} \quad 3.14$$

where f is the focal length, NA is the numerical aperture, θ is the full divergence angle, and a is the fiber core diameter.

F. FILTERS

When the power signal falls on the photodiode, photocurrent will be generated in the photodiode. This photocurrent is given by equation 3.15 [10]:

$$i_{ph}(t) = \frac{\eta q}{h\nu} P(t) \quad 3.15$$

where η is the quantum efficiency of the photodiode, q is the electron charge, and $P(t)$ is the total power incident on the photodiode. This total power includes the wanted signal and the noise, which is the unwanted power signal. The primary sources of noise in a PIN photodiode are the shot noise and Johnson noise. The total current noise generated in a PIN photodiode is given by [19] the following:

$$i_n^2 = \sqrt{2q(i_{sig} + i_{bkg} + i_0)\Delta f + \frac{4kT\Delta f}{R_{eq}}} \quad 3.16$$

where i_{sig} is the dc current caused by the signal flux, i_{bkg} is the current resulting from background, i_0 is the dark current, R_{eq} is the equivalent resistance for the photodiode circuit, and Δf is the receiver bandwidth. As seen from equation 3.16, the noise in a PIN photodiode depends on the receiver bandwidth, where the noise can be reduced by narrowing the bandwidth of the receiver, which can be done by using a narrow band pass filter. In this thesis, the filter used has part number *FL1300-30 – Laser Line Filter*. Figure 21 shows the transmission characteristics of this filter. This filter has a Central Wavelength (CWL) = 1300nm ±6, and Full Width Half Maximum (FWHM) = 30nm ±6 [18].

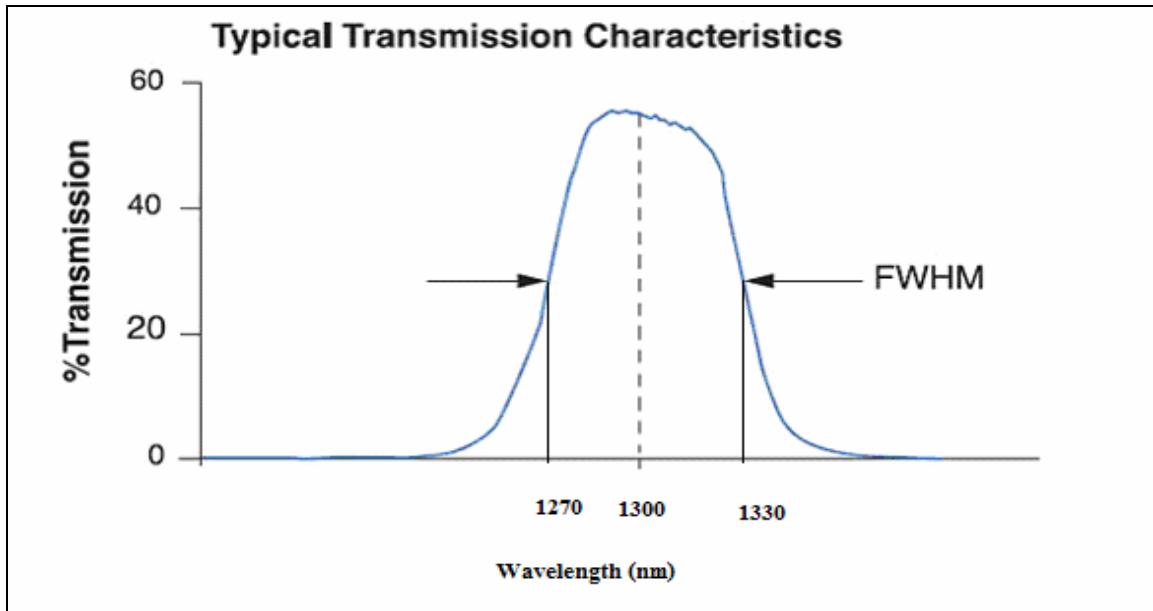


Figure 21. Typical Transmission Characteristics *FL1300-30 – Laser Line Filter* (After Ref. [17]).

G. LASER SAFTY

Lasers are light sources that produce highly concentrated power that can cause serious biophysical effects on the skin or eyes. The level of laser effects, of course, depends on its incident power and wavelength. These laser injuries may occur from direct incident or reflected beams.

Lasers with wavelengths below 700nm and above 1400nm may cause serious damage to the outer layers of the eye and may cause skin burns. Lasers with wavelengths from 400 to 1400nm can penetrate deeply into the eye and reach the retina, the sensitive part of the eye that transfers visual information to the brain, where the rays of light will be focused and in turn will cause a μm burn spot on the Retina. This small spot has 100,000 times the effect than at the eye surface.

Several laser safety standards have been issued, and since then, they are reviewed from time to time to update them. Below are the main standards:

- IEC825-1: Equipment classification, requirements and user's guide.
- ANSI Z136.1: American National Standard for the safe use of lasers.

- CDRH: Center for Devices and Radiological, federal Performance for laser products.
- IRPA1991: Guidelines on human exposure to laser radiation.

The classification of laser safety is widely agreed upon, but there are slight differences in the classification scheme. IEC, which is the most used, uses Arabic numerals and uppercase letters. CDRH uses Roman numerals and lower case letters, and ANSI uses Arabic numerals and lower case letters [20]. The classification is given below [20]:

- Class1: this is a very low radiated power (up to 0.4mW), or completely enclosed and cannot be viewed so that it is considered to be safe.
- Class 2: this includes visible low-power (from 0.4-1mW) lasers with wavelengths of 400-700nm. This class is eye-safe if viewed for less than 0.5 seconds.
- Class 3A: this class produces hazards if viewed with magnifying instruments or if the incident power per unit area exceeds 25w/m^2 . This includes visible lasers with power up to 500mW and invisible lasers with power up to 2mW.
- Class3B: this class produces eye hazards if viewed directly, while its reflections are safe. The maximum power limit for this class is 0.5W.
- Class4: this class is unsafe because it can produce eye and skin hazards if exposed directly to it or to its reflections. It may also produce fire hazards by interacting with flammable materials.

THIS PAGE INTENTIONALLY LEFT BLANK

IV. HISTORICAL OVERVIEW AND SUMMARY OF WORK DONE IN REF. [1]

The design of the system was started in a previous thesis (see Ref. [1]), in which a preliminary design of a Free-Space Optics (FSO) communication system has been developed and tested using commercial off the shelf (COTS) components. The work can be summarized as follows:

- a. Modification of the ML6652RDK media converter. This media converter originally comes with an Agilent HFBR-5103 transceiver and operates at wavelengths of 1300nm, with output power of 0.04mW (-14dB). The transceiver was removed and a 1x9 connector was left in order to be used for other higher power transceivers, as shown in Figure 22.



Figure 22. Modified ML6652RDK Media Converter (From Ref. [1]).

- b. Transceivers have been purchased from Lasermate Group, Inc. They have 1mW (0dB) of output power. These transceivers have been connected to the modified media converter using a 1x9 connector.
- c. An initial FSO link was established between two adjacent modified media converters as shown in Figure 23.

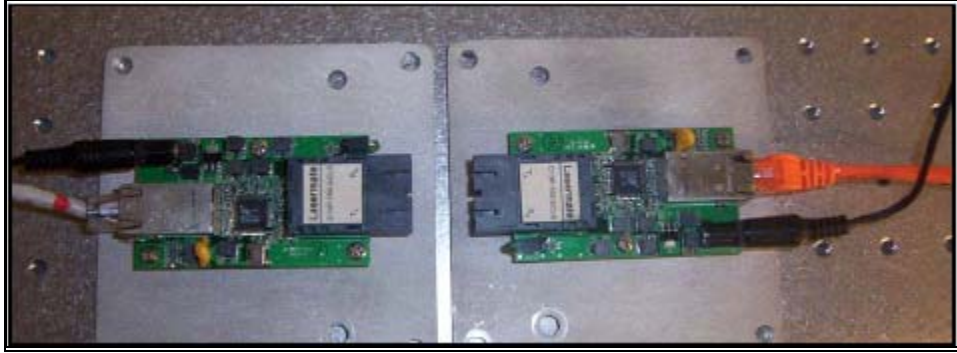


Figure 23. Initial FSO Link (From Ref. [1]).

- d. Short fiber optics cables and lenses have been connected to the transceivers and the FSO link was established for a distance of 5ft, as shown in Figure 24.

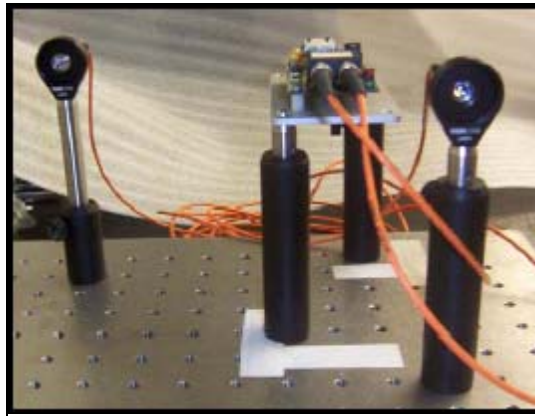


Figure 24. Transceivers With Fiber Optics and Lenses to Establish FSO Link Over a 5ft Distance (From Ref. [1])

- e. Measurement for the output power of one of the transceivers has been taken, which showed that a 0.11mw signal could be detected at 300ft.

V. DESIGN IMPROVEMENT

This chapter covers the work done in this thesis to improve the FSO system design.

A. STARTING POINT

In order to establish a starting point for testing, and to ensure that all the design components were working properly as described in [1], the test in Figure 24 was repeated with and without using the lenses for the receiver side.

First, the two transceivers, without lenses connected to the receiver, were located close to each other (2cm apart) and the link was tested. The distance between the two was increased gradually (5cm each time) and the link was tested repeatedly until a 5ft distance was reached between the two transceivers. The same was done for the two transceivers with lenses connected to the receiver. The FSO worked properly.

The alignment was very difficult to achieve in both cases, but it was relatively easier with the lenses connected to the transceivers than it is without the receiver's lenses because the light is gathered by a comparatively large lens instead of trying to aim a laser beam into a detector of active area around $75\mu\text{m}$. Alignment between lenses and fibers should be handled carefully, otherwise the beam will be lost and will not reach the detector.

The beam alignment process was difficult due to the following:

- The alignment was done manually. Trying to aim a laser with unknown beam spread into a miniscule detector area of about $75\mu\text{m}$ was near impossible.
- This was complicated by the fact that the beam was not visible (1310nm). The only way to know that the two systems were aligned was to observe the link connect LED on the media converter. When it illuminated, alignment had been achieved.

The problem with this technique was that the LED would not illuminate until the transceivers had already communicated with each other, negotiated the bit rate, and the link had been established. This created an unreasonable time delay.

In order to satisfy the objective of this thesis, three main issues were taken into consideration:

- Transmitter output power: the transmitter output power should be high enough to reach the required distance. In [1], power measurement showed that the power of the existing transceivers could be detected at a distance of 300ft. These measurements were taken without using a filter, so that it was not known whether the detected signal, at the 300ft range, is the wanted signal or just noise. The power measurements beyond the 300ft distance were not known. It was decided to test the existing transceivers and see what maximum distance could be achieved. Then, based on the test results, it would be decided on how much transmitting power is need for farther distances.
- Collimated transmitter beam: in order for the beam to reach a larger distance with sufficient power and acceptable spread, the laser beam should be highly collimated to be able to focus sufficient power on the detector (receiver). Collimators of part number F260FC-C and diameter of about 7mm (see **Error! Reference source not found.**) were selected to start with.
- Beam Spread measurements: In order to gain knowledge about the beam width, measurements of the beam width or spread should be done.

B. STEPS TO EXTEND RANGE AND TESTING

To gain knowledge about how the laser beam spreads over a distance, extensive measurements were taken in the lab for the laser beam width originating from the laser transceiver. A photo-detector connected to a multimeter was used to measure the received voltage. The measurements were taken in the lab with the equipment set up as shown in Figure 25.

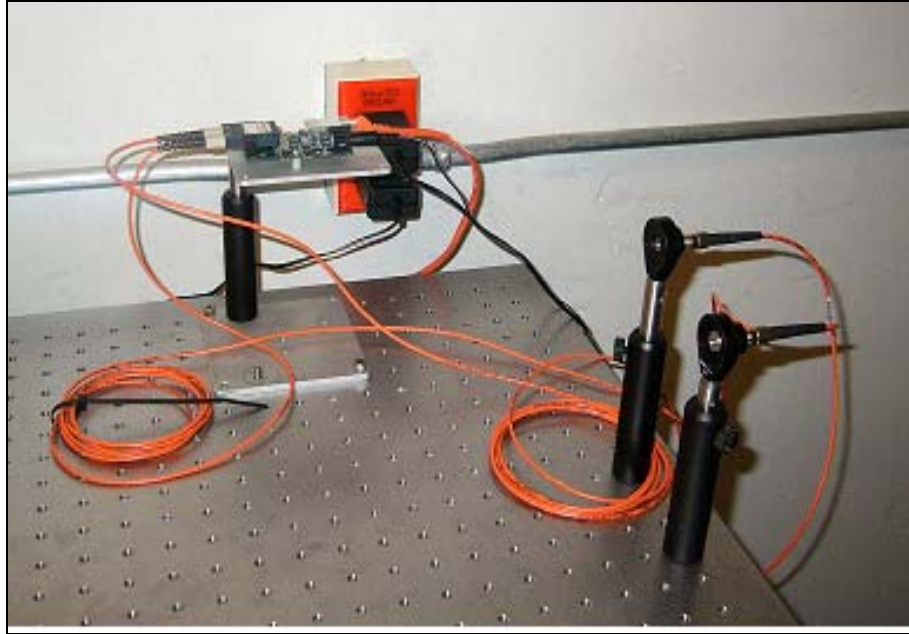


Figure 25. The FSO System is Anchored on the Test Bench.

A filter, FL1300-30, was placed in front of the InGaAs photodetector during the measurement process to eliminate any external noise. The measurements are included in Chapter VI. The results showed that the laser beam spread over about 20mm horizontal distance with barely enough power to be detected by the receiver at a 5ft distance. Although there was relatively high power originating from the transmitter, the laser beam was diverging rapidly and spread over a relatively large area at the receiver location resulting in low light irradiance. Actually, the laser beam was not collimated enough to reach the receiver with high irradiance. The receiver was working near the threshold values. In order to get the best collimated beam out of the collimator lens, the transmitting fiber needed to be adjusted carefully with the collimator lens. This was difficult to do without using an assisting device to see the beam spot. At this point, the need for a sensitive infrared viewer arose. Infrared viewer model 7215 was used later and a good collimated beam with a narrow beam waist could be obtained for larger distances.

In order to be able to go farther distances, beyond the test bench, the two systems were mounted on two tripods as shown in Figure 26. Testing was started at a 3m distance between the two systems.

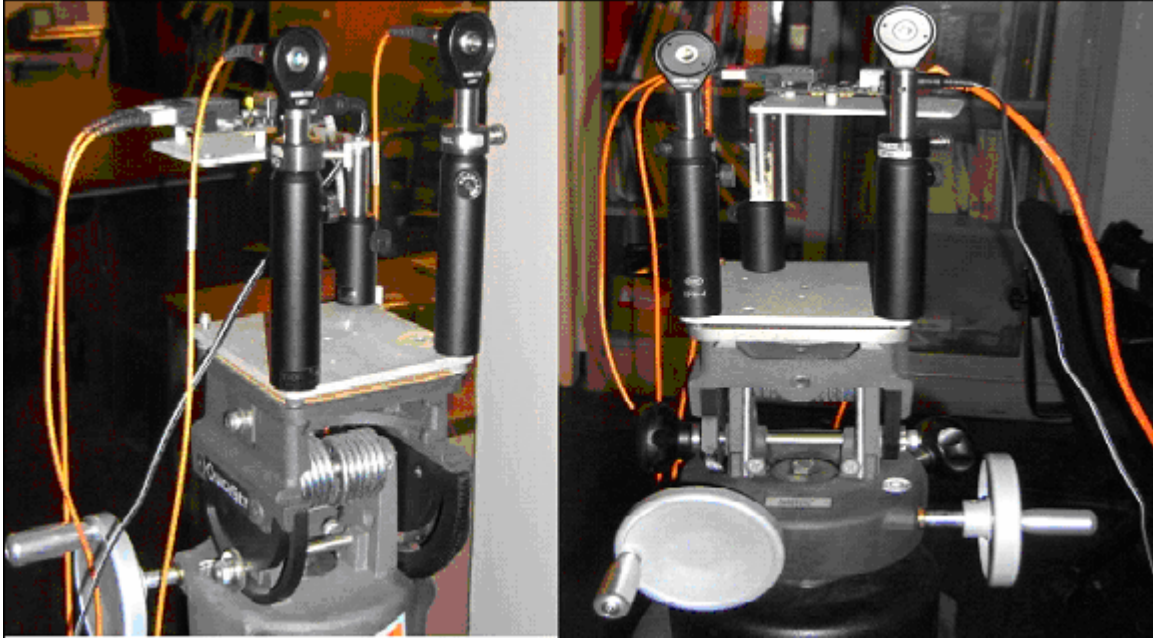


Figure 26. The Two FSO Systems were Mounted on Tripods.

The alignment became much more difficult than it was in the bench test, because there were more degrees of freedoms to move. An infrared viewer (electroviewer model 7215 from Electrophysics Corporation) was used to see the beam spot location. The link was established and measurements for voltage/power were taken and are included in Chapter VI.

Even though the beam can be seen by the infrared viewer, the alignment was still very difficult and time consuming, because height, elevation, beam angle and side movements need to be taken into account. The most difficult to adjust among all these variables was the rotational adjustment when the transmitter needed to be rotated to aim directly at the receiver lens. This was difficult because a slight rotation for the transmitter lens would result in a large movement, for the beam spot, in the receiver location. In order to rotate the transmitter more precisely the design was slightly modified to include a mechanical rotational movement for the transmitter. This addition is shown in Figure 27.



Figure 27. The Two Systems on Tripods With the Mechanical Rotational Added.

The alignment process was repeated for a 5m distance between the two systems and the link was successfully established. Power measurement was taken at this distance and beam spot was captured using the infrared viewer and digital camera. The power measurements and the beam spot for the 5m distance are included in Chapter VI. The alignment was still difficult and time consuming. Adjusting the alignment, between the fiber and the transmitting lens, needed to be done precisely by moving the fiber in and out from the lens to obtain the best collimated beam, otherwise the irradiance would decrease rapidly over distance and the beam spot would disappear after a short distance even if there was enough power out from the transmitter lens.

At a 10m distance, the beam spots for both transmitters were distorted and spread widely over a relatively large area. This was expected because multimode fibers were used for the transmitters. The multimode fiber has a relatively large diameter with respect to the operating wavelength, which allows many modes to propagate through the fiber creating an output beam with a large waist and relatively high divergence angle (i.e., see equations 3.9 and 3.10). These propagating modes produce constructive and destructive interference among them. This results in the formation of bright and dark light spots called speckles, which in turn, would result in non-uniformly distributed power at the receiver location. In

order to eliminate this problem and to reduce the light speckles, a single mode fiber is used for both transmitters. The link was successfully established for 10m and 15m distances. Power measurements, photos and measurements for the beam spot in both cases (multimode and single mode fibers) are shown in Chapter VI.

The maximum distance that could be achieved in the laboratory was 15m. For larger distances the equipment was moved to the corridor in the basement of Spanagel Hall. Before moving the equipment, the maximum range that might be achieved and the threshold receiver voltages were calculated in advance. The advance calculation showed that that maximum range that would be achieved using the available collimator/focuser and a 1mW transmitter was from 40m to 50m. Since we are using an InGaAs photodiode to measure the voltages, the voltage that would be measured in front of the receiver lens was calculated to be between 178mV and 211mV for the maximum range. The detailed calculation is included in Chapter VI. First the two systems were placed 30m apart and the link was successfully established between them; then the distance was doubled to 60m. At 60m the link could not be established, so the distance was decreased gradually until the link was successfully established at a 40m distance between the two FSO systems. Voltage/power measurements for 30m and 40m are included in Chapter VI. The irradiance of the beam spot at 30m and 40m was too low to be captured or measured.

In order to measure the delay produced by the free-space optics (FSO) system, two laptops were connected directly through a crossover cable. Different sizes and types of files were transferred between the two laptops. The two laptops were then connected via the FSO system and the same files were transferred again between the two laptops. The measured time periods for both cases were compared and no major delay was noticed. The result of these tests is included in Chapter VI.

In order to measure how much time the system takes to reestablish the link, the beam was interrupted and the time needed to establish the link was measured for 5m, 10m, 15m, and 30m distances. It takes the system 17 seconds to negotiate the bit rate and complete the link establishment.

VI. RESULTS AND CONCLUSIONS

This chapter includes the results of the tests and measurements done in the frame of this thesis, and the conclusions obtained are based on these measurements and tests.

A. RESULTS

1. Beam Width Measurement

In order to gain knowledge about how the laser beam spreads over a distance, extensive measurements were taken in the lab for the laser beam width originating from the laser transceiver and received by the photodetector connected to a multimeter. The measurements were taken in the lab where the transmitter and the photodetector are anchored on the test bench. A filter of 1310nm was used during the measurement process to eliminate any external noise. The measurements could not have been taken over distances beyond 5ft because this was the limit of the test bench.

The following equipment and devices were used in the test:

1. InGaAs Detector with the following characteristics:

- Detector: InGaAs PIN.
- Spectral Response: 700-1800nm.
- Peak Wavelength: 1500nm +/-50nm.
- NEP: $1 \times 10^{-14} \text{ W}/\sqrt{\text{HZ}}$.
- Rise/Fall Time: 5ns.
- Diode Capacitance: 22pF.
- NEP: $5 \times 10^{-14} \text{ W}/\text{HZ}^{1/2}$.
- Dark Current: 25nA @ -12V.
- Active Area: 1mm^2 (0.8mm^2).
- Linearity Limit: 1mW.
- Max reverse current: 10mA.
- Damage Threshold: 100mW CW.
- Operating Temp: 0 to 85°C.

The responsivity of this detector, for any wavelength, can be obtained from Figure 28.

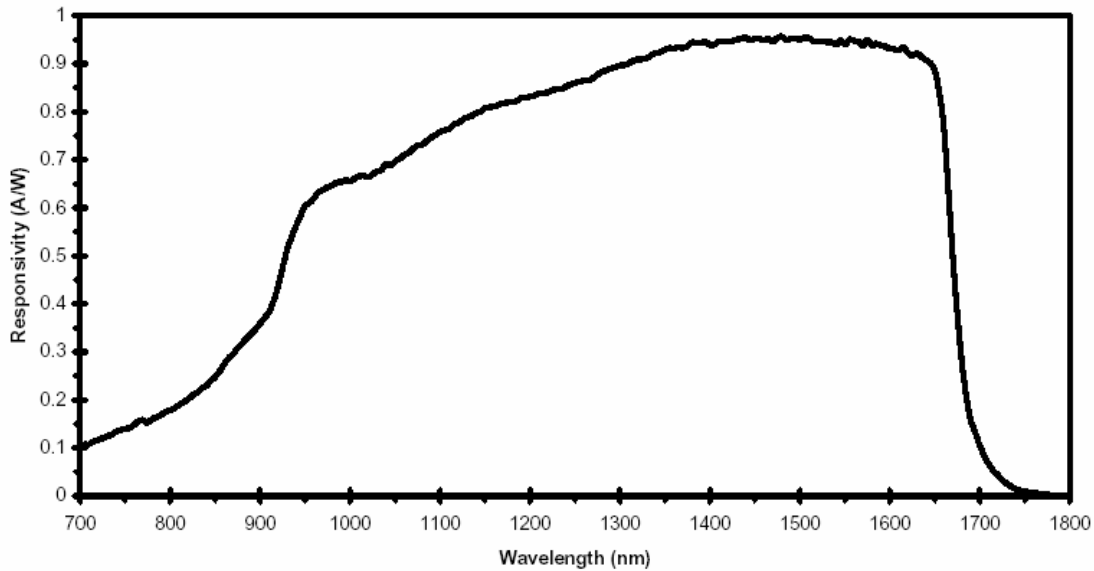


Figure 28. Responsivity vs. Wavelength for InGaAs Detector (From Ref. [17])

2. FL1300-30 Laser Line Filter, CWL=1300nm \pm 6nm and Full Width Half Maximum (FWHM)=30nm \pm 6nm (Thorlabs, Inc.).
3. Transmitter: Lasermate Group, Inc. transceiver C13F-155-SCL5: 1310nm, MQW laser diodes, output power -5-0dBm, receiver sensitivity of less than -30dB, and supply voltage 5V.
4. Digital multimeter.

The data measurements were taken over distances, between detector and transmitter, of 4mm, 1ft, 2ft, 3ft, 4ft, and 5ft. The transceiver was connected to the media converter. The test arrangement is shown in Figure 29, and the data measurements are shown in Tables 4-9.

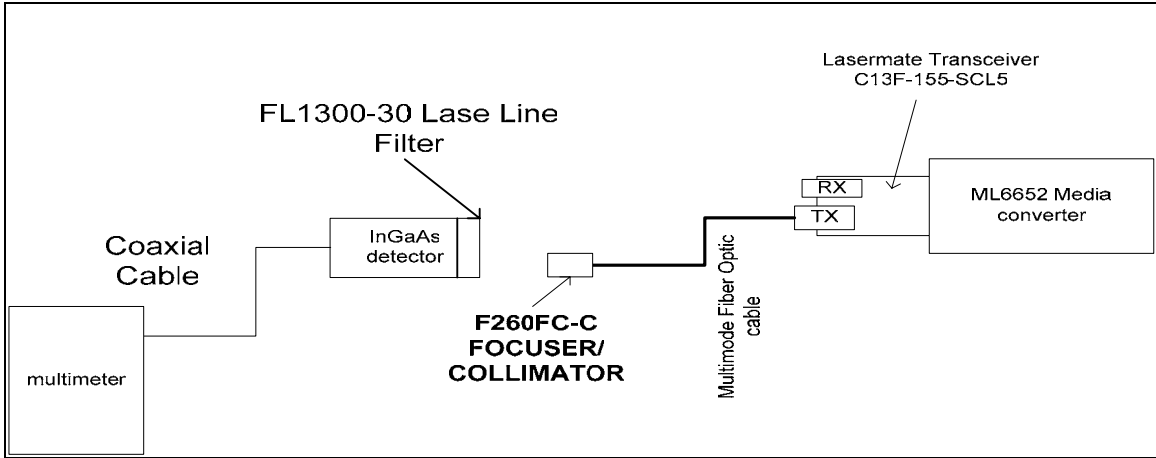


Figure 29. Test Arrangement for Beam Width Measurement

Figure 30 was used to find the corresponding current for each voltage measured, and equation 4.1 was used to calculate the power, where \mathfrak{R} is the photodetector responsivity. From Figure 28, the responsivity for InGaAs photodiode at a 1310nm wavelength was found to be $\mathfrak{R} = 0.88 \text{ A/W}$.

$$P_p = \frac{I_p}{\mathfrak{R}(\lambda)} \quad 4.1$$

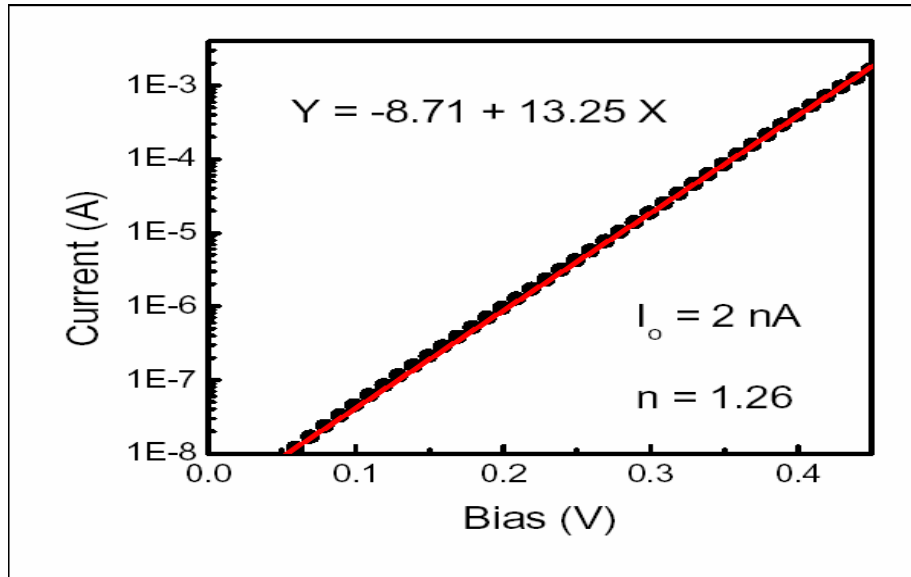


Figure 30. I-V Characteristics for the InGaAs Photodiode (From Ref. [1]).

Distance from the center of the beam (mm)	Voltage (v)	Distance from the center of the beam (mm)	Voltage (v)	Distance from the center of the beam (mm)	Voltage (v)	Distance from the center of the beam (mm)	Voltage (v)
-24	0.001	-13	0.055	-2	0.254	8	0.205
-23	0.001	-12	0.049	-1	0.258	9	0.201
-22	0.001	-11	0.075	0 (at the center of the beam)	0.391	10	0.15
-21	0.001	-10	0.188	1	0.287	11	0.088
-20	0.001	-9	0.188	2	0.248	12	0.048
-19	0.001	-8	0.192	3	0.228	13	0.048
-18	0.001	-7	0.196	4	0.206	14	0.037
-17	0.001	-6	0.198	5	0.212	15	0.02
-16	0.002	-5	0.202	6	0.209	16	0.003
-15	0.014	-4	0.213	7	0.209	17	0.002
-14	0.034					18	0.001

Table 4. Beam Width Measurement Data for 4mm Distance Between the Transmitter and Detector.

Distance from the center of the beam (mm)	Voltage (v)	Distance from the center of the beam (mm)	Voltage (v)	Distance from the center of the beam (mm)	Voltage (mm)
-66	0.001	-5	0.203	14	0.005
-61	0.004	-4	0.215	15	0.005
-39 to -60	0.005	-3	0.240	16	0.003
-31 to -38	0.004	-2	0.248	17	0.002
-20 to -30	0.003	-1	0.270	18 to 25	0.001
-19	0.003	0 (at the center of the beam)	0.276	25 to 59	0.001
-18	0.003	1	0.258	61	0.00
-17	0.005	2	0.233		
-16	0.010	3	0.215		
-15	0.033	4	0.212		
-14	0.068	5	0.208		
-13	0.111	6	0.208		
-12	0.159	7	0.207		
-11	0.190	8	0.204		
-10	0.193	9	0.192		
-9	0.194	10	0.149		
-8	0.197	11	0.083		
-7	0.195	12	0.045		
-6	0.200	13	0.011		

Table 5. Beam Width Measurement Data for 1ft Distance Between the Transmitter and Detector.

Distance from the center of the beam (mm)	Voltage (v)	Distance from the center of the beam (mm)	Voltage (v)	Distance from the center of the beam (mm)	Voltage (mm)
67	0.001	-5	0.209	16	0.003
-45 to 60	0.005	-4	0.215	17	0.002
-30 to 44	0.004	-3	0.219	18	0.002
-23 to 29	0.003	-2	0.226	19	0.001
-22	0.004	-1	0.232	20 to 67	0.001
-21	0.006	0 (at the center of the beam)	0.236	21	0.000
-20	0.012	1	0.230		
-19	0.021	2	0.223		
-18	0.034	3	0.215		
-17	0.052	4	0.206		
-16	0.072	5	0.202		
-15	0.087	6	0.196		
-14	0.110	7	0.190		
-13	0.130	8	0.181		
-12	0.146	9	0.161		
-11	0.169	10	0.140		
-10	0.181	11	0.102		
-9	0.192	12	0.072		
-8	0.201	13	0.052		
-7	0.202	14	0.017		
-6	0.203	15	0.008		

Table 6. Beam Width Measurement Data for 2ft Distance Between the Transmitter and Detector.

Distance from the center of the beam (mm)	Voltage (v)	Distance from the center of the beam (mm)	Voltage (v)	Distance from the center of the beam (mm)	Voltage (mm)
70 to 74	0.001	-5	0.200	21	0.003
- 68 to 70	0.002	-4	0.208	22	0.002
-30 To -67	0.003	-3	0.209	23	0.002
-29	0.004	-2	0.210	24	0.002
-28	0.006	-1	0.211	25 to 100	0.001
-27	0.009	0 (at the center of the beam)	0.211		
-26	0.013	1	0.208		
-25	0.021	2	0.202		
-23	0.035	3	0.200		
-22	0.045	4	0.197		
-21	0.055	5	0.184		
-20	0.064	6	0.174		
-19	0.077	7	0.167		
-18	0.092	8	0.153		
-17	0.111	9	0.142		
-16	0.125	10	0.127		
-15	0.140	11	0.107		
-14	0.148	12	0.089		
-13	0.158	13	0.072		
-12	0.164	14	0.058		
-11	0.169	15	0.046		
-10	0.178	16	0.034		
-9	0.186	17	0.022		
-8	0.188	18	0.014		
-7	0.189	19	0.010		
-6	0.193	20	0.006		

Table 7. Beam Width Measurement Data for 3ft Distance Between the Transmitter and Detector.

Distance from the center of the beam (mm)	Voltage (v)	Distance from the center of the beam (mm)	Voltage (v)	Distance from the center of the beam (mm)	Voltage (mm)
-76 to -77	0.001	-9	0.189	21	0.018
-40 to -75	0.002	-8	0.195	22	0.014
-37 to -39	0.003	-7	0.198	23	0.01
-36	0.004	-6	0.199	24	0.006
-35	0.006	-5	0.198	25	0.004
-34	0.08	-4	0.197	26	0.003
-33	0.010	-3	0.192	27	0.002
-32	0.014	-2	0.193	28 to 150	0.001
-31	0.017	-1	0.195		
-30	0.024	0 (at the center of the beam)	0.201		
-29	0.029	1	0.195		
-28	0.035	2	0.191		
-27	0.045	3	0.190		
-26	0.058	4	0.192		
-25	0.071	5	0.193		
-24	0.078	6	0.190		
-23	0.083	7	0.180		
-22	0.090	8	0.169		
-21	0.103	9	0.149		
-20	0.118	10	0.135		
-19	0.137	11	0.125		
-18	0.149	12	0.111		
-17	0.155	13	0.102		
-16	0.161	14	0.090		
-15	0.165	15	0.079		
-14	0.169	16	0.067		
-13	0.177	17	0.055		
-12	0.182	18	0.039		
-11	0.184	19	0.031		
-10	0.185	20	0.024		

Table 8. Beam Width Measurement Data for 4ft Distance Between the Transmitter and Detector.

Distance from the center of the beam (mm)	Voltage (v)	Distance from the center of the beam (mm)	Voltage (v)	Distance from the center of the beam (mm)	Voltage (mm)
-37 to -200	0.001	-7	0.163	21	0.038
-36	0.002	-6	0.168	22	0.032
-35	0.002	-5	0.172	23	0.025
-34	0.003	-4	0.174	24	0.016
-33	0.005	-3	0.180	25	0.013
-32	0.006	-2	0.182	26	0.010
-31	0.010	-1	0.186	27	0.007
-30	0.014	0 (at the center of the beam)	0.188	28	0.005
-29	0.018	1	0.184	29	0.003
-28	0.025	2	0.183	30	0.002
-27	0.034	3	0.180	31	0.001
-26	0.044	4	0.177	32 to 75	0.001
-25	0.0054	5	0.180	76	0.00
-24	0.065	6	0.183		
-23	0.072	7	0.182		
-22	0.077	8	0.17		
-21	0.078	9	0.158		
-20	0.083	10	0.140		
-19	0.093	11	0.127		
-18	0.103	12	0.118		
-17	0.120	13	0.105		
-16	0.125	14	0.098		
-15	0.128	15	0.092		
-14	0.132	16	0.083		
-13	0.135	17	0.076		
-12	0.142	18	0.066		
-11	0.152	19	0.056		
-10	0.158	20	0.047		

Table 9. Beam Width Measurement Data for 5ft Distance Between the Transmitter and Detector.

Based on the data in the previous tables, Figure 31 was generated. Figure 31 shows that the beam spread over a relatively large distance from the center of the beam. The power decreased rapidly from 0.364mW to about 0.738 μ m over a 5ft distance. This rapid decrease of power was due to the relatively large divergence angle, which results in

a large geometric loss (i.e., beam spread). The two systems were operating at the threshold voltages and the beam was not a good collimated beam. At this point, the need for a sensitive infrared viewer became evident. The infrared viewer was very helpful in locating the beam spot and adjusting the distance between the fiber and the collimator to get the smallest output beam waist. A better collimated beam was obtained when the infrared viewer was used, as will be shown in the next section.

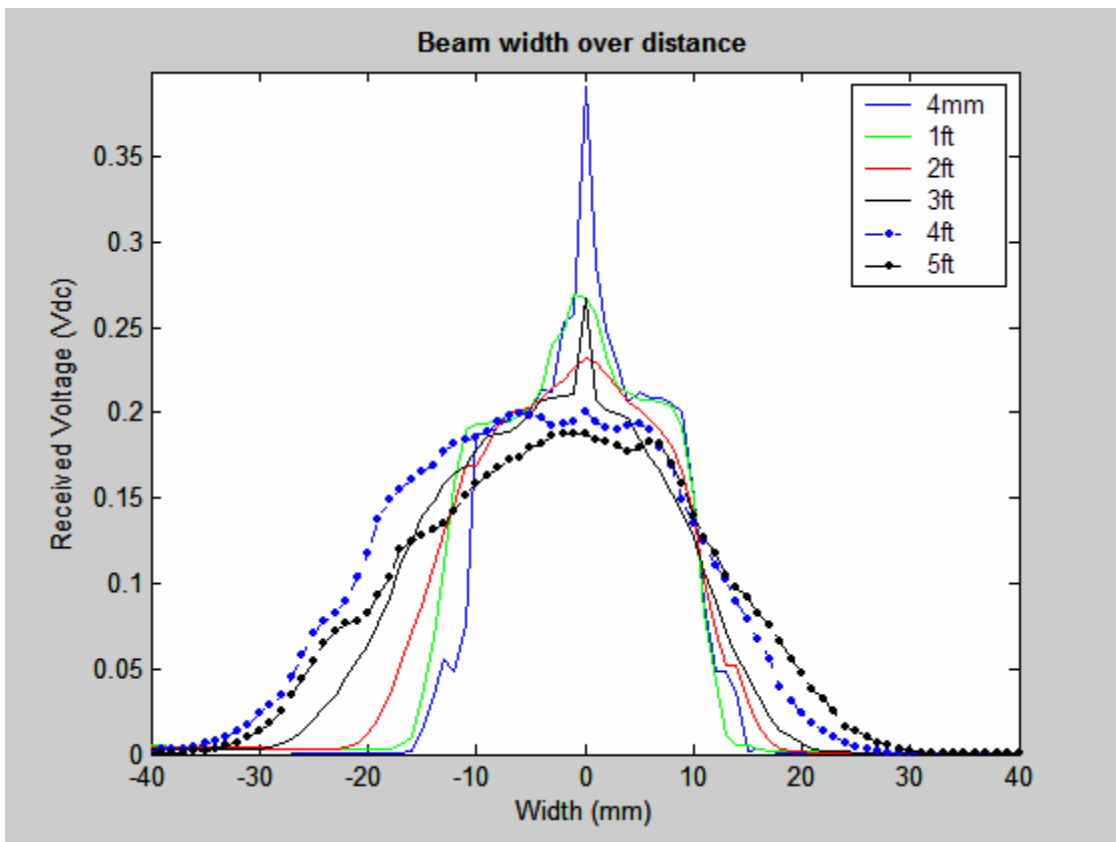


Figure 31. Beam Width Measurement.

2. Voltage/Power and Beam Spot Measurements

With the two transceivers aligned 5ft apart, and with the link “up and running” on the bench table, voltage/power measurements were taken at different system locations. A digital multimeter and detector were used in these measurements. The measurements have been taken with the filter mounted in front of the detector. The measurement locations are shown in Figure 32.

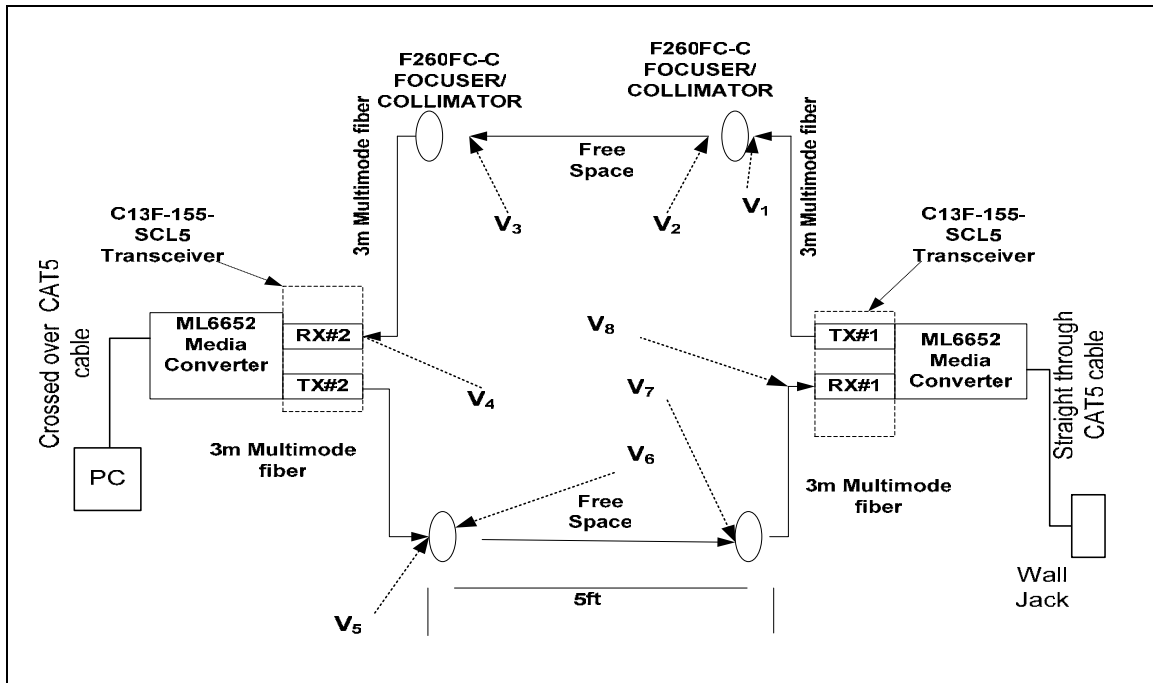


Figure 32. Test Locations for 5ft Distance

- V_1 was measured at the end of the multimode fiber before transmitting lens #1.
- V_2 was measured right at the output of the transmitting lens.
- V_3 was measured right before the receiving lens of receiver #2.
- V_4 was measured at the end of the fiber cable before receiver #2.
- V_5 was measured at the end of the multimode fiber before the transmitting lens #2.
- V_6 was measured right at the output of transmitting lens #2.
- V_7 was measured right before the receiving lens of receiver #1.
- V_8 was measured at the end of the fiber cable before receiver #1.

The four lenses used were identical. These lenses, from Thorlabs, Inc. with Part No. F260FC-C, are factory aligned using a single mode fiber to collimate/focus the light from or onto the fiber optic. Figure 33 shows this type of lenses.

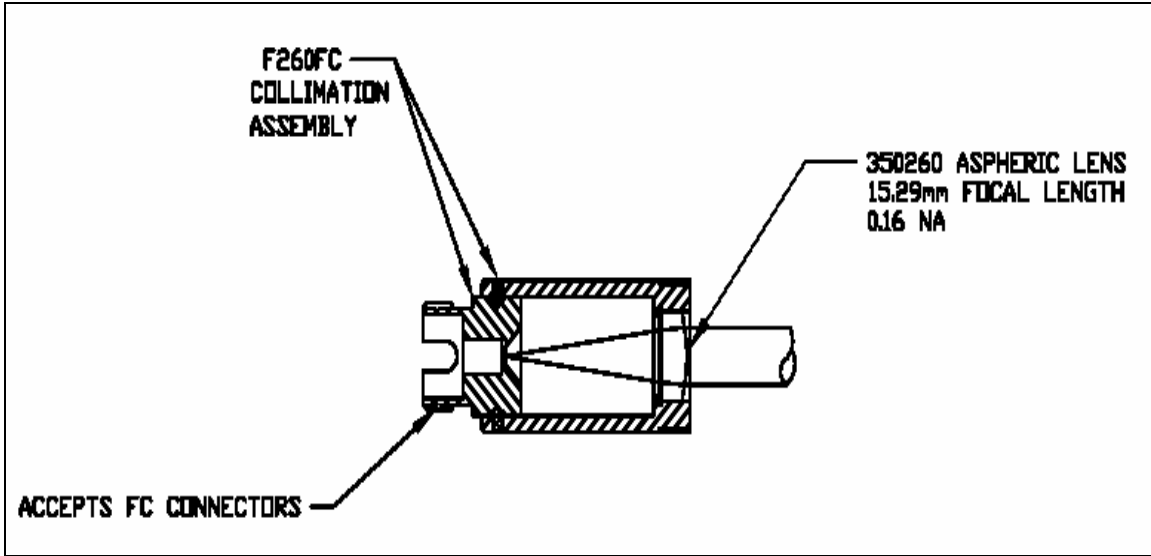


Figure 33. F260FC-C Collimator/Focuser (After Ref. [17]).

The results of the measurements are shown in Table 10.

Voltage \ Distance	3m	
	V(V)	P(mW)
V ₁ & P ₁	0.437	1.1
V ₂ & P ₂	0.395	0.34
V ₃ & P ₃	0.348	0.0.085
V ₄ & P ₄	0.315	0.0.034
V ₅ & P ₅	0.432	1.02
V ₆ & P ₆	0.397	0.4
V ₇ & P ₇	0.346	0.091
V ₈ & P ₈	0.311	0.031

Table 10. Voltage Measurements for 5ft (1.524m) Distance.

The corresponding current for each voltage was obtained from Figure 30, and hence the power was calculated using equation 4.1 with $\Re = 0.88$ A/w.

It was noticed that there was enough power at the receiver; however, there was a considerable amount of coupling loss between the fiber and the collimator/focuser and

also between the fiber and the TOSA/ROSA. Multimode fiber optic cables of 1m and 3m were used between the receiver and the collimator/focuser. However, no major difference was noticed in the power measured at the output of the cables. To maximize the coupling efficiency, the fiber was adjusted by slightly moving it in and out from the lens until the maximum voltage was obtained at the receiver location.

To test the system over larger distances, the two systems were mounted on tripods as shown in Figure 27. To prepare for the file transfer measurements, the two media converters were connected to two laptops with static IP configuration as shown in Figure 34.

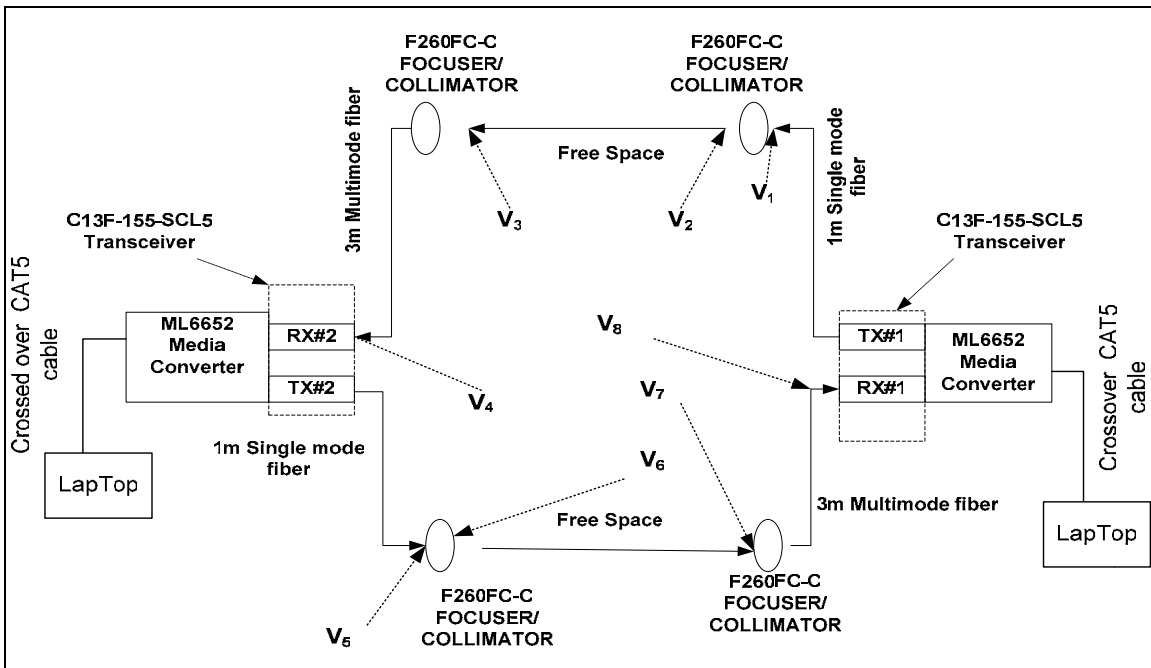


Figure 34. Test Configuration/Voltage Locations for 3m and Larger Distances

The test was started with a 3m distance between the two FSO systems. Then the distance was increased to 5m. The link between the two systems was established successfully at bit rate of 100Mbps as indicated by the LED on the media converter. Voltage measurements were taken using the same multimeter and InGaAs detector used in the measurements at 5ft.

To show how much noise was removed by the filter, the measurements were performed with and without the filter mounted in front of the detector. The voltage measurements are shown in Table 11.

Distance		3m		5m	
		V(V)	P(mW)	V(V)	P(mW)
V₁ & P₁	Wo/filter	0.437	1.1	0.437	1.1
	W/filter	0.430	0.95	0.430	0.95
V₂ & P₂	Wo/filter	0.395	0.34	0.395	0.34
	W/filter	0.390	0.3	0.390	0.3
V₃ & P₃	Wo/filter	0.378	0.284	0.375	0.28
	W/filter	0.345	0.091	0.340	0.074
V₄ & P₄	Wo/filter	0.360	0.142	0.353	0.102
	W/filter	0.318	0.045	0.317	0.042
V₅ & P₅	Wo/filter	0.432	1.02	0.432	1.02
	W/filter	0.429	1.0	0.432	1.0
V₆ & P₆	Wo/filter	0.397	0.4	0.397	0.4
	W/filter	0.392	0.37	0.392	0.37
V₇ & P₇	Wo/filter	0.365	0.199	0.360	0.176
	W/filter	0.342	0.090	0.330	0.058
V₈ & P₈	Wo/filter	0.355	0.113	0.341	0.96
	W/filter	0.318	0.045	0.315	0.036

Table 11. Voltage Measurements With and Without the Filter Over 3m and 5m Distances.

It can be seen from the above measurements that the filter helped in removing a relatively large amount of noise from the receiving signal. This removed noise was about 10% of the received signal.

At 10m and larger distances the link was successfully established after replacing the multimode fiber with a single mode fiber for the transmitters. This is described in the

next paragraphs. The voltage measurements at the 10m distance with multimode and single mode are shown in Table 12.

Distance		10m	
		V(V)	P(mW)
V ₁ & P ₁	W/multimode	0.437	1.1
	W/single mode	0.416	0.795
V ₂ & P ₂	W/multimode	0.395	0.34
	W/single mode	0.385	0.318
V ₃ & P ₃	W/multimode	0.298	0.023
V ₄ & P ₄	W/multimode	0.285	0.015
V ₅ & P ₅	W/multimode	0.432	1.02
	W/single mode	0.410	0.7
V ₆ & P ₆	W/multimode	0.397	0.4
	W/single mode	0.378	0.284
V ₇ & P ₇	W/multimode	0.287	0.016
V ₈ & P ₈	W/multimode	0.268	0.0091

Table 12. Voltage Measurements With Multimode and Single Mode Cables Used for Both Transmitters for 10m.

The voltage measured at the end of the receiving fiber (V₄ and V₈) was still above the threshold voltage for the receiver.

The distance was increased farther and the link was successfully established, without any problems, for 15m. This was the largest distance that could be tested in the lab. Then it was decided to move the equipment to the corridor in the basement of Spanagel Hall. Before moving the equipment to the corridor, a maximum distance

calculation was performed as detailed in the next section. The FSO link was successfully established at 30m and 40m distances. In order to measure the effect of using the filter at these ranges, the measurements were done with and without the filter. The measurements are shown in Table 13. From these measurements the removed noise was calculated to be 12% of the total received signal.

Distance \ Voltage		15m		30m		40m	
		V(V)	P(mW)	V(V)	P(mW)	V(V)	P(mW)
V ₁ & P ₁	Wo/filter	0.416	0.795	0.416	0.795	0.416	0.795
	W/filter						
V ₂ & P ₂	Wo/filter	0.385	0.318	0.385	0.318	0.385	0.318
	W/filter						
V ₃ & P ₃	Wo/filter	0.299	0.023	0.265	0.0083	0.240	0.00398
	W/filter	0.267	0.0085	0.230	0.00255	0.222	0.00228
V ₄ & P ₄	Wo/filter	0.285	0.015	0.242	0.0044	0.193	0.000625
	W/filter	0.265	0.0089	0.232	0.0023	0.158	0.000284
V ₅ & P ₅	Wo/filter	0.410	0.7	0.410	0.7	0.410	0.7
	W/filter						
V ₆ & P ₆	Wo/filter	0.378	0.284	0.378	0.284	0.378	0.284
	W/filter						
V ₇ & P ₇	Wo/filter	0.295	0.018	0.265	0.0089	0.245	0.0045
	W/filter	0.260	0.0068	0.233	0.0022	0.215	0.002
V ₈ & P ₈	Wo/filter	0.283	0.014	0.253	0.0054	0.212	0.0017
	W/filter	0.268	0.0091	0.220	0.002	0.172	0.000454

Table 13. Voltage Measurements With and Without Using a Filter Over 15m, 30m, and 40m Distances.

At each distance, the beam spot size was captured and measured. The beam spot, for 3m and 5m distances, was captured using an infrared viewer and digital camera. The beam spot measurements are shown in Figure 35 and Figure 36. The beam spot

measurements showed that the beam was spread over an area that has a vertical axis longer than the horizontal axis because the divergence angle θ_{\perp} is larger than θ_{\parallel} , which is a normal characteristic of FP laser beams (see Figure 9). The beam at these distances was still a collimated beam.

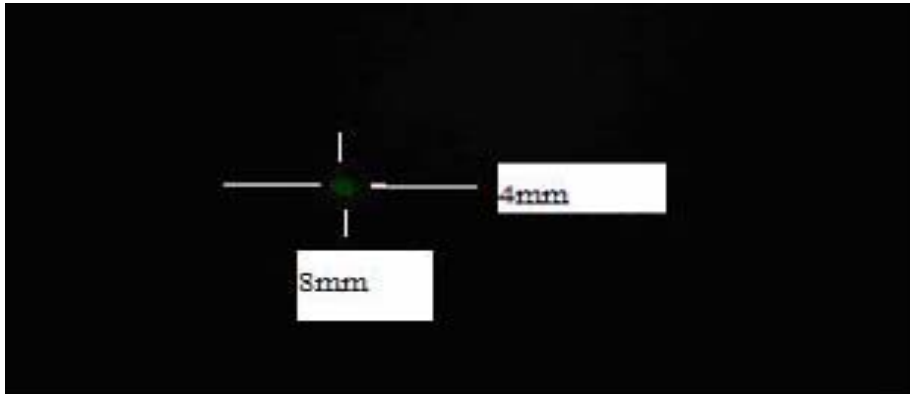


Figure 35. Beam Spot for 3m Distance

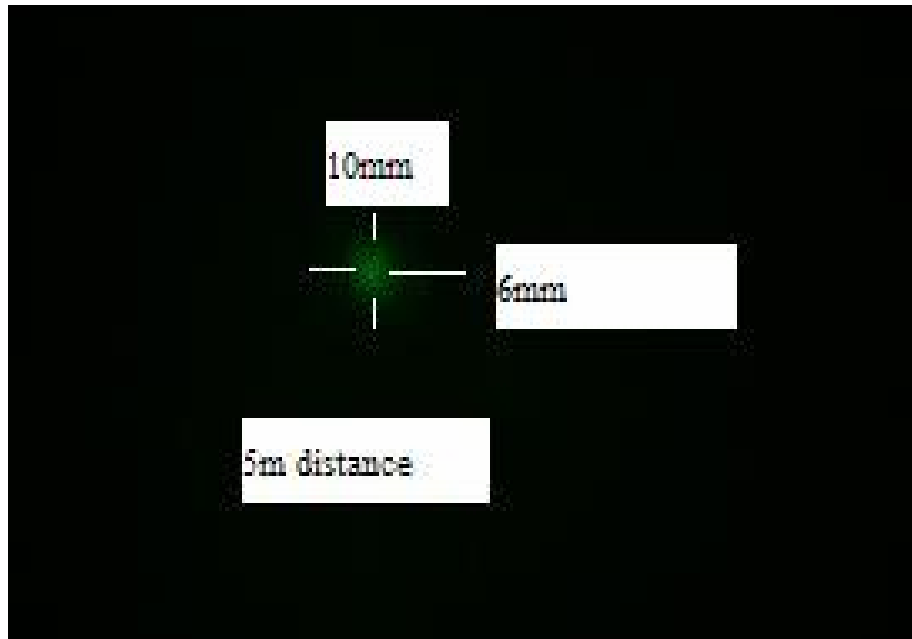


Figure 36. Beam Spot for 5m Distance.

Then the distance was increased to 10m between the two systems. In the beginning, the link could not be established for this distance. The back LED (yellow

color LED) was flashing, indicating that there was data present at the receive side. However, the LED in front of the media converter (i.e., LED for the successful negotiated bit rate) never lit and the link could not be established. To investigate and solve this problem, voltage/power measurements were performed at a 10m distance between the two systems. The measurements showed that there was enough power received at the end of the fiber optic cable (i.e., V_4 and V_8). The beam spots for both transmitters were captured using an infrared viewer and digital camera, as shown in Figure 37.

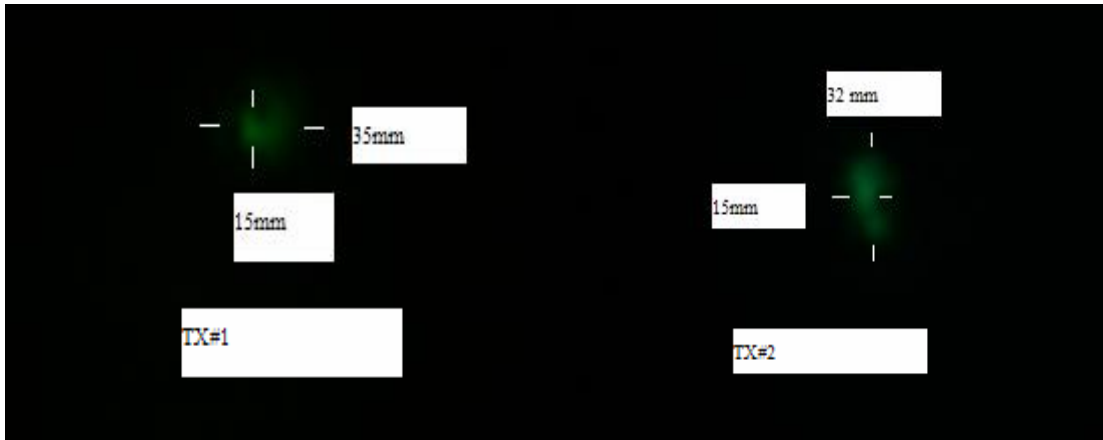


Figure 37. Beam Spots for the Two Transmitters at 10m Using a Multimode Fiber Optic Cable.

The beam spot at this distance was not distributed uniformly, the divergence angle got extremely large and the light spot was scattered and distorted. The beam spots for the two transmitters were spread over undefined shapes of size greater than 15mm by 30mm. This was because of the interference among the modes propagating in the multimode fiber, which resulted in a “mess” of modes and distorted signals at the receiver location. This signal could not be recognized by the receiver. To get a better collimated beam, single fiber optic cables were used between the transmitter and the collimators for both transmitters. The output power from the transmitting lens was degraded very little; however, the resultant beam spots for both transmitters were uniformly distributed over circles of diameters less than 10mm. The beam spots for the two transmitters, after using a single mode fiber, are shown in Figure 38.

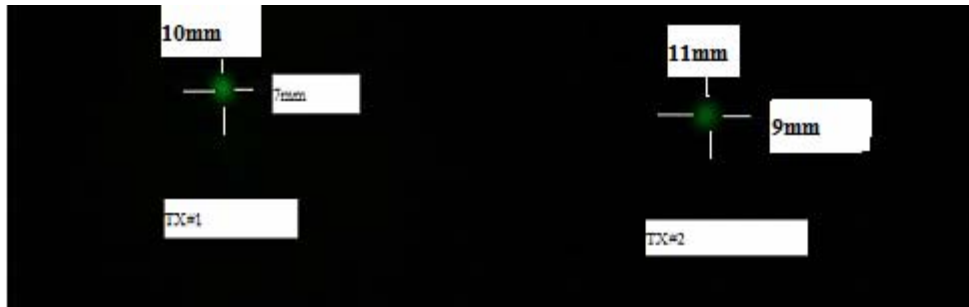


Figure 38. Beam Spot for the Two Transmitters at 10m Distance Using a Single Mode Fiber.

The beam spot at a 15m distance is shown in Figure 39 for both transmitters. The beam spots were spread over larger circles with diameters of 13mm and 14mm.

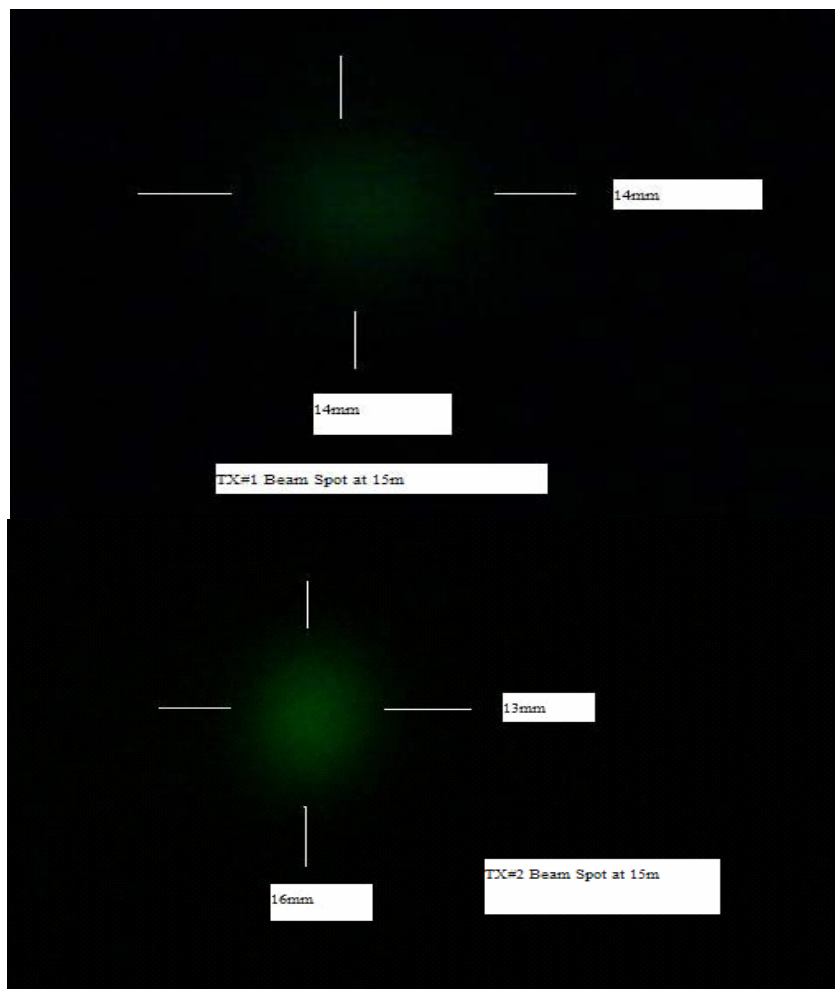


Figure 39. Beam Spot for the Two Transmitters at 15m Distance.

3. FSO Delay Time Measurements

To measure how much delay is produced by the free-space optic (FSO), two laptops with static IP configurations were connected using a crossover cable. One of the laptops was considered a server and the other a client. The file transfer always occurred from the server to client. Shared files of different types (pdf, doc, and pp) and sizes were used for comparison purposes. Later the two laptops were connected via the FSO system and the same shared files were transferred from the server to the client at different distances using a 100Mbps bit rate. Time measurements are shown in Table 14 and illustrated in Figure 40.

The file transfer was done five times and the average time was calculated. This time includes not only the transfer time, but also the time it takes to process the file in the server and the client. The delay time introduced by the FSO system can be obtained by subtracting the direct time from FSO time.

From Table 14, it is clear that there is no real difference between the process/transfer time for direct connection and the FSO connections.

File Size	Average process/Transfer Time				
	Direct connection via crossover UTP	Two Laptops connected via FSO.			
		10m	15m	30m	40m
27.2 MB PDF File	16.25 sec	16.5 sec	16.5 sec	17sec	16.75 sec
41.3MB pp File	110.5 sec	111.75 sec	110.25 sec	111.5 sec	111.25 sec
90.2MB doc File	8.25 sec	9 sec	8.25 sec	9.5 sec	8
182 MB doc File	19 sec	20.5 sec	20.75 sec	18.25 sec	20

Table 14. Average Process/Transfer Time for Different File Types and Sizes.

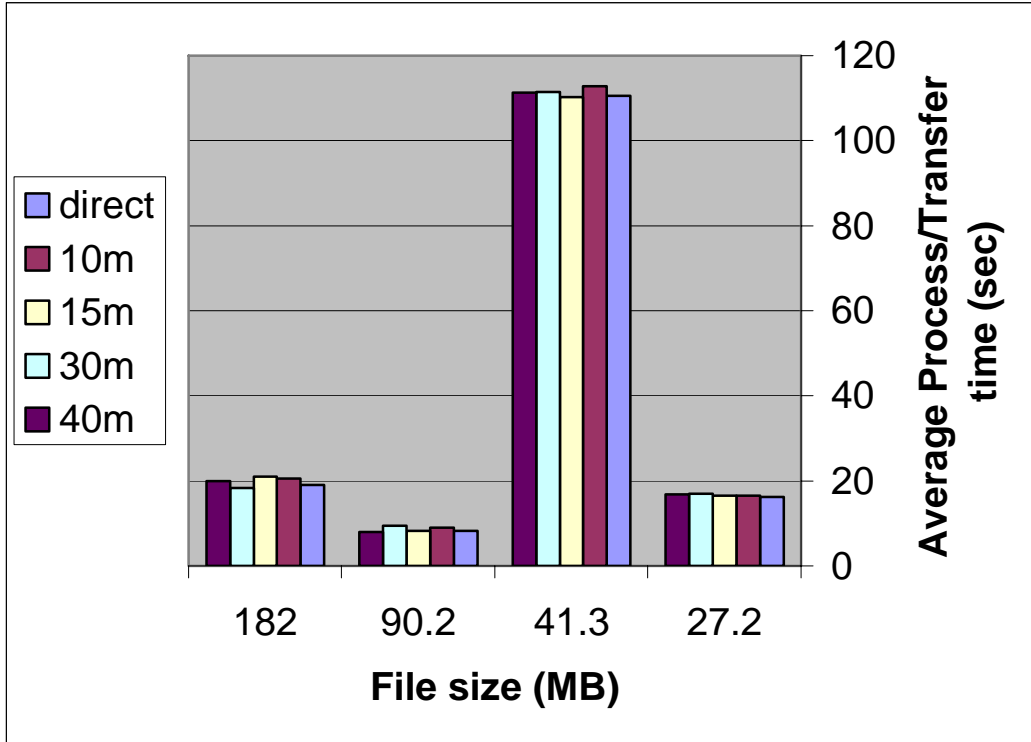


Figure 40. File Process/Transfer Time.

4. Maximum Range Calculation for the Existing FSO System

Before testing the system for larger distances, the maximum achievable range was calculated.

The receiver sensitivity is -30dB, using 1mW as a reference, so that the minimum power (P_{in}) that can be detected by this receiver is:

$$-30dB = 10 \log \frac{P_{in}}{1mW} \Rightarrow P_{in} = 1\mu W .$$

It was assumed that the coupling efficiency between the fiber and the ROSA was 65% (which is the average coupling efficiency for the 1x9 transceiver), then the minimum power at the end of the receiving fiber using the notation in Figure 32 was obtained as:

$$P_{4min} = P_{8min} = \frac{1 \times 10^{-6} \times 100}{65} \cong 1.54\mu W .$$

The coupling efficiency between the receiver lens (focuser) and the fiber was assumed to be 75% (see Chapter III, Section C). Then the minimum power that should be collected by the focuser lens would be:

$$P_{3\min} = P_{7\min} = \frac{1.54\mu W \times 100}{75} \cong 2.05\mu W .$$

Based on the power measurements along the corridor in [1], the atmospheric attenuation was calculated for ranges of 100ft, 120ft, 140ft, 160ft, 180ft, and 200ft using equation 3.6, and the average value was taken to give $\alpha = 0.0092 m^{-1}$.

The following parameters were calculated for a 30m distance. The output power from the transmitter's collimator is usually less than 1mW because of the single fiber losses, coupling efficiency (see Chapter III, Section C), and the fluctuation of the laser output power. The transmitter output power was assumed to be 0.318mW as in Table 13 (P_2 or P_6).

The total power that would be received at 30m was calculated from equation 3.6:

$$P_R = P_T e^{-\alpha R} = 0.318 \times 10^{-3} e^{-0.0092 \times 30} = 241\mu W .$$

The fraction of the power that would be collected by the focuser was obtained using equation 3.7:

$$P_R = P_T \frac{A_{receiver}}{(\theta R)^2} e^{-\alpha R}$$

where $\theta = \frac{1}{2} \times 0.035^\circ = 0.0175^\circ = 0.3054 mrad$, $A_{receiver} = \pi \times \left(\frac{BD}{2}\right)^2$ is the area of the receiver aperture (the area of the focuser aperture), and BD is the maximum beam diameter that can be focused properly by the lens/focuser. The divergence angle (θ), numerical aperture (NA), the output beam diameter, and the focal length (f) are the parameters for the collimator/focuser F260FC-C (see Figure 20). BD was calculated as:

$$BD = 2w_o \cong 2.74mm .$$

Then

$$A_{receiver} = \pi \times \left(1.37 \times 10^{-3}\right)^2 = 5.9 \times 10^{-6} m^2 .$$

And by substituting these values into equation 3.7:

$$P_R = P_T \frac{A_{receiver}}{(\theta R)^2} e^{-\alpha R} = 0.318 \times 10^{-3} \frac{5.9 \times 10^{-6}}{\left(0.3054 \times 10^{-3} \times 30\right)^2} e^{-0.0092 \times 30} = 17 \mu W$$

The power at the end of the receiving fiber, assuming 75% coupling efficiency, was calculated as:

$$P = 17 \mu W \times 0.75 = 12.75 \mu W .$$

Then the power that might be received by ROSA, assuming 65% coupling efficiency, was calculated:

$$P = 12.75 \mu W \times 0.65 = 8.3 \mu W .$$

Since we were using a photodiode to measure the voltage in front of the receiving lens, it is also useful to calculate this voltage in advance. The photodiode has 0.88mm² active area, so that equation 3.7 was used again to calculate the power that would be collected by this photodiode at 30m as follows:

$$P_R = P_T \frac{A_{receiver}}{(\theta R)^2} e^{-\alpha R} = 0.318 \times 10^{-3} \frac{0.88 \times 10^{-6}}{\left(0.3054 \times 10^{-3} \times 30\right)^2} e^{-0.0092 \times 30} \cong 2.5 \mu W .$$

This power was converted to current using equation 4.1:

$$I_p = P_p \times \mathfrak{R} = 2.5 \times 10^{-6} \times 0.88 = 2.2 \times 10^{-6} A .$$

From Figure 30 this current corresponds to $V \approx 245mV$. Also the Spot Size at 30m was calculated using equation 3.4:

$$w(z) = \frac{\lambda}{\pi w_0} z = \frac{1310 \times 10^{-9}}{\pi \times 1.37 \times 10^{-3}} \times 30 = 9.1mm ,$$

which means that the beam spot diameter was 18.2mm. All the above calculations were repeated for 40m, 50m, and 60m. These parameters are shown in Table 15 and Figure 41. These calculations showed that the threshold power that might be collected by ROSA is reached at distances between 40 and 50m.

Range (m)	Spot Size (mm)	Beam Spot Diameter (mm)	Total received power (μW)	Power collected by Focuser (μW)	Expected Power at the end of the receiving fiber(μW)	Expected Power that might be collected by ROSA (μW)	Voltage measured with 0.88mm^2 photodiode located in front of the receiving lens (mV)
30	9.1	18.2	241	17	12.75	8.3	245
40	12.17	24.34	220	8.7	6.5	4.2	211
50	15.22	30.44	200	5	3.75	2.43	178
60	18.26	36.52	183	3.2	2.4	1.56	165

Table 15. Advance Calculations to Estimate the Maximum Range for Existing System

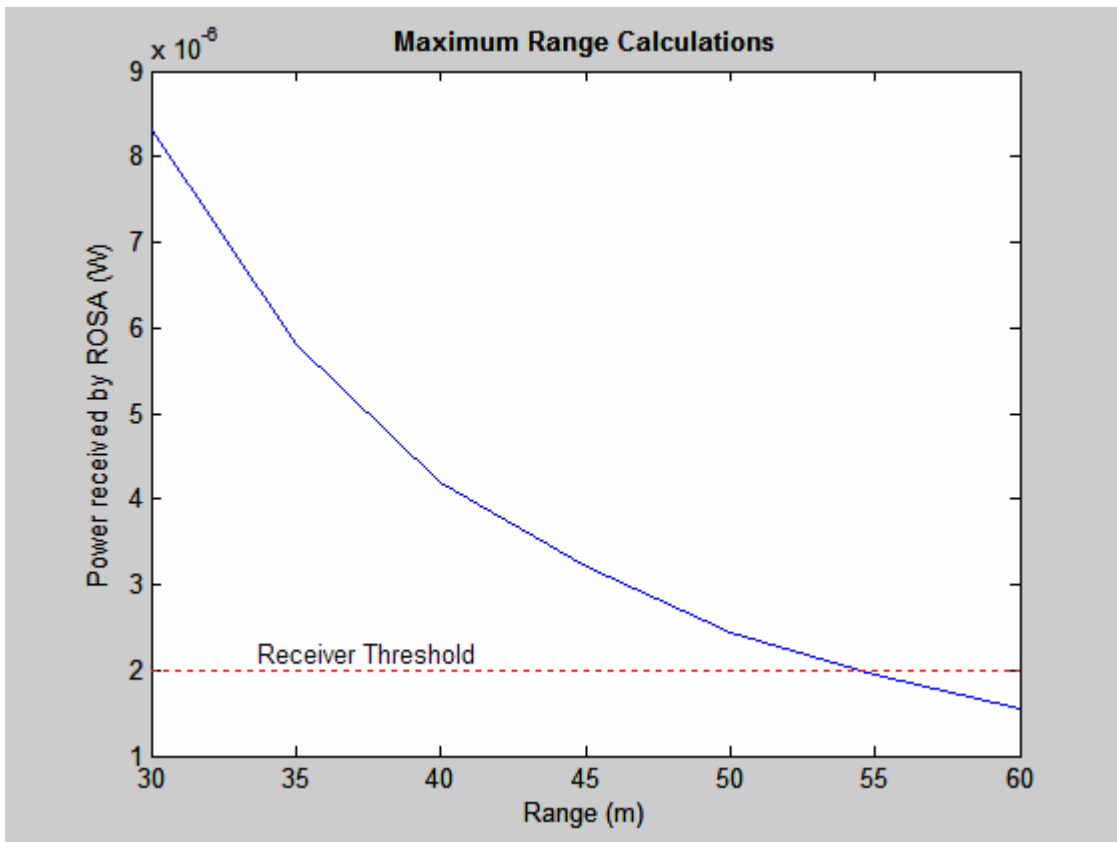


Figure 41. Maximum Range Calculation for the Existing FSO System.

5. Maximum Range Calculation for 3mW Transmitter

It was hard to find a 1x9 transceiver with output power larger than 3mW. Thus, it is useful to calculate in advance the maximum range that would be achieved if a 3mW transmitter was used with the existing optics (i.e. F260FC-C collimator). If we assume that the receiver sensitivity is -30dB (1μm), and by taking into account the fiber losses and coupling efficiencies, the power that should be collected by the lens/focuser and focused on the fiber, can be calculated as follows:

$$P_{3\text{or}7\text{min}} = \frac{1\mu\text{W} \times 100 \times 100}{75 \times 65} = 2.04\mu\text{m}.$$

Since the transmitter output power is always less than the declared maximum output power, for the reasons mentioned in the above section, it was assumed that the output power was 2.2mW. The calculations in the previous section were repeated for distances of 100m, 120m, 140m, 160m, and 180m. The results of the calculations are included in Table 16 and Figure 42.

R (m)	Spot Size (mm)	Beam Spot Diameter (mm)	Total received power (μW)	Power collected by Focuser (μW)	Expected Power at the end of the receiving fiber(μW)	Expected Power that might be collected by ROSA (μW)	Voltage measured with 0.88mm ² photodiode located in front of the receiving lens (mV)
80	24.3	48.6	1054	10.4	7.8	5.1	210
100	30	60	876.7	5.5	4.125	2.7	185
120	36.5	73	729.4	3.2	2.4	1.56	175
140	42.6	85.2	606.81	1.96	1.47	0.96	159

Table 16. In Advance Calculations to Estimate the Maximum Range for a 3mW Transmitter.

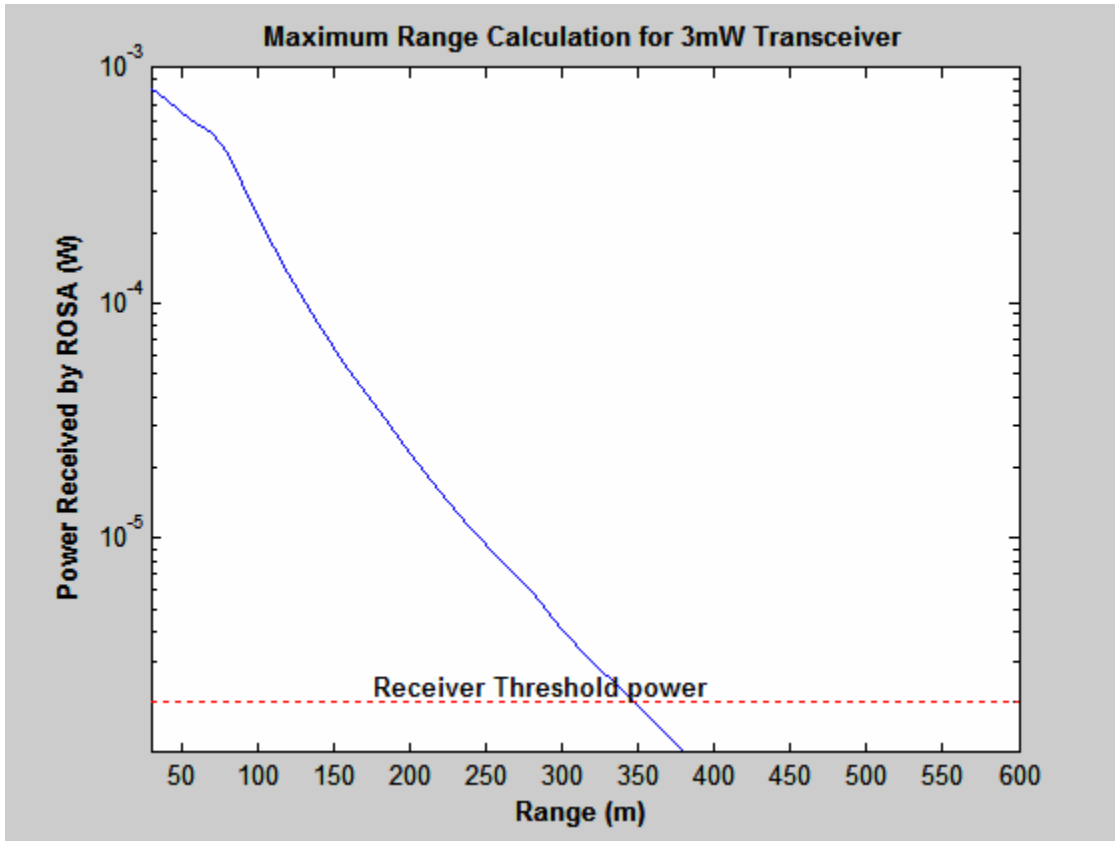


Figure 42. Maximum Range Calculation for 3mW Transceiver.

It can be seen that there is relatively large power at the receiver location; however, the irradiance is low due to the beam spread. Due to the relatively low irradiance, the focuser will collect a small portion of the received power, which will limit the maximum range that will be achieved.

It appears, from Table 16, that the maximum achievable range is less than 120m. However, if a larger focuser is used for the receiver, the maximum range could be extended further. Calculations were done assuming that a 1-inch focuser was used in the receiver side. The area of the receiver was calculated to be:

$$A_{receiver} = \pi \times (12.7 \times 10^{-3})^2 = 506.7 \times 10^{-6} m^2 .$$

The calculations in the previous section were repeated here for distances from 80m to 380m. The results of the calculations are included in Table 17.

R (m)	Spot Size (mm)	Beam Spot Diameter (mm)	Total received power (μ W)	Power collected by Focuser (μ W)	Expected Power at the end of the receiving fiber (μ W)	Expected Power that might be collected by ROSA (μ W)
80	24.3	48.6	1054	894.57	670.9	436
100	30	60	876.7	476.3	357.225	232.2
120	36.5	73	729.4	275.2	206.4	134.16
140	42.6	85.2	606.81	168.19	126.14	82
160	48.7	97.4	504.82	107	80.34	52.2
180	54.8	109.6	420	70.41	52.8	34.32
200	60.9	121.8	349.4	47.45	35.6	23.1
220	67	134	290.67	32.62	24.5	15.9
240	73	146	241.8	22.81	17.1	11.12
260	79	158	201.2	16.17	12.12	7.9
280	85.2	170.4	167.4	11.6	8.7	5.7
300	91.3	182.6	139.24	8.4	6.3	4.1
320	97.4	194.8	115.84	6.1	4.61	3
340	103.5	206.4	94.37	4.5	3.4	2.2
360	109.6	219.2	80.17	3.4	2.52	1.64
380	115.7	231.4	66.7	2.51	1.9	1.22

Table 17. In Advance Calculations to Estimate the Maximum Range for a 3mW Transmitter and a 1-inch Receiver Focuser.

Based on these results, it is clear that the range can be extended by using a higher power transmitter and a large focuser. By using a 1mW transmitter and a 1-inch focuser in the receiver side, a maximum range between 300m to 340m could be achieved.

B. CONCLUSION

The author concludes that the 500m range could be achieved by using a low power 5mW transmitter with a small 50mm focuser. However, the most challenging problem is to facilitate the alignment process and to keep the systems aligned in a real working environment. This could be done by using a more powerful transmitter and larger collimators so that the beam would spread over a wide area at the receiver location with enough power to be detected by the receiver, or by using precise auto alignment and a tracking system. If this was accomplished in a cost effective way, the FSO device would be a competitive device to the commercially available FSO systems.

THIS PAGE INTENTIONALLY LEFT BLANK

LIST OF REFERENCES

- [1] Perera, Janaka P., *A low-cost man-portable free space optics communication device for Ethernet applications*, thesis, Naval Postgraduate School, December 2004.
- [2] Pedrotti, Frank L., S. J. Leno and S. Pedrotti, *Introduction to optics*, 2nd ed, pp. 491-494, Prentice Hall, New Jersey, 1993.
- [3] Laser Bit Space Optics, <http://www.systemsupportolutions.com/laserbit.htm>, last accessed October 2005.
- [4] Willebrand, H. A., and B. S. Ghuman, *Fiber Optics Without Fiber*, IEEE Spectrum 38,8 (August 2001).
- [5] Neo, Soo Sim Daniel, *Free Space Optics communication for mobile military platforms*, thesis, Naval Postgraduate School, December 2003.
- [6] Timus, Oguzhan, *Free Space Optics communication for Navy surface ship platforms*, thesis, Naval Postgraduate School, March 2004.
- [7] Garcia, Gillbert O., and David C. Joseforsky, *Transformational communications architecture for the unit operations center (UOC)Common Aviation Command and Control system (CAC2S); and Command and control On-the-move Network, Digital Over the horizon Relay(CoNDOR)*, thesis, Naval Postgraduate School, June 2004.
- [8] Info Security Writers, <http://www.infosecwriters.com/hhworld/hh9/roc/node2.html>, last accessed October 2005.
- [9] OPTEK Technology, OPF5101 technical data sheet, <http://www.optekinc.com/pdf/OPF5101.pdf>, last accessed October 2005.

- [10] Keiser, Gerd, *Optical Fiber Communications*, third edition, McGraw-Hill, 2000.
- [11] University of Glasgow, U.K,
<http://www.physics.gla.ac.uk/Optics/Lectures/ModernOptics/ModOpt2001.pdf>, last accessed October 2005.
- [12] System Support Solution Inc., MN, USA.
<http://www.systemsupportolutions.com/whitepapers/Physics%20of%20Free-space%20Optics.pdf>, last accessed October 2005.
- [13] Cunnighah, David G., and William G. Lane, *Gigabit Ethernet Networks*, Macmillan Technical Publishing, USA, 1999.
- [14] <http://www.fiber-optics.info/fiber-history.htm>, last accessed October 2005.
- [15] Black, Uyles, *Optical Networks third generation transport system*, pp. 40-42, Prentice Hall, New Jersey, 2002.
- [16] Wilson, John, and John Hawkes, *Optoelectronics an introduction*, 3rd edition, pp. 375-376, Prentice Hall, Great Britain, 1998.
- [17] Thorlabs, Inc., <http://www.thorlabs.com>, last accessed October 2005.
- [18] OZOptics, <http://www.ozoptics.com>, collimator/focuser data sheet, last accessed October 2005.
- [19] Dereniak, E. L., and G. D. Boreman, *Infrared Detectors and Systems*, John Wiley & Sons, 1996.
- [20] Henderson, A. Roy, *A guide to laser safety*, 1st edition, Chapman & Hall, 1997.

INITIAL DISTRIBUTION LIST

1. Defense Technical Information Center
Ft. Belvoir, Virginia
2. Dudley Knox Library
Naval Postgraduate School
Monterey, California.
3. Professor Gamani Karunasiri
Department of Physics
Code PH/Kg
Naval Postgraduate School
Monterey, California
4. Professor Richard Harkins
Department of Physics
Code PH/Hr
Naval Postgraduate School
Monterey, California
5. Mr. Mark Lasher
Advanced Technology Branch
Code 2853
SPAWAR Systems Center San Diego
San Diego, California
6. LCDR. Mohammad Alrasheedi
Royal Saudi Naval Forces
Riyadh, Saudi Arabia